A Theory of Multi-Scale, Curvature-Based Shape Representation for Planar Curves

Farzin Mokhtarian and Alan K. Mackworth+

Technical Report 89-14
August 1989

Department of Computer Science
University of British Columbia
Vancouver, B.C.
Canada V6T 1W5

+ Fellow, Canadian Institute for Advanced Research

Abstract

This paper presents a multi-scale, curvature-based shape representation technique for planar curves which satisfies several criteria, considered necessary for any shape representation method, better than other shape representation techniques. As a result, the representation is suitable for tasks which call for recognition of a noisy curve of arbitrary shape at an arbitrary scale or orientation.

The method rests on the concept of describing a curve at varying levels of detail using features that are invariant with respect to transformations which do not change the shape of the curve. Three different ways of computing the representation are described in this paper. These three methods result in three different representations: the curvature scale space image, the renormalized curvature scale space image, and the resampled curvature scale space image.

The process of describing a curve at increasing levels of abstraction is referred to as the *evolution* of that curve. Several evolution properties of planar curves are described in this paper. Some of these properties show that evolution is a physically plausible operation and characterize possible behaviours of planar curves during evolution. Some show that the representations proposed in this paper in fact satisfy some of the required criteria. Others impose constraints on the location of a planar curve as it evolves. Together, these evolution properties provide a theoretical foundation for the representation methods introduced in this paper.

1. Introduction

This paper introduces a novel theory of multi-scale, curvature-based shape representation for planar curves. It should be pointed out that only the problem of representing the shape of a planar curve which has been extracted from an image or input by a user has been addressed in this paper. We believe the problem of extracting such a curve from an image, the *segmentation problem*, is a separate problem and should not be considered to be part of the shape representation problem [Saund 1989].

Some of the results presented in this paper have appeared elsewhere but this paper is our first comprehensive treatment of multi-scale representation techniques.

A useful shape representation method in computational vision should make accurate and reliable recognition of an object possible. Therefore such a representation should necessarily satisfy a number of criteria [Haralick *et al* 1989]. The following is a list of such criteria:

a. Efficiency: The representation should be efficient to compute and store. This

is important since it may be necessary for an object recognition system to perform real-time recognition. By *efficient* we mean that the computational complexity should be a low-order polynomial in time and space.

b. Invariance: Uniform scaling, rotation and translation are considered to be the transformations which do not change the shape of an object. Therefore the representation should remain essentially invariant while the represented object undergoes one of these transformations.

c. Sensitivity: The degree of change to the shape of an object should correspond to the degree of the resulting change in its representation. Otherwise, a small change to the shape of an object may cause a large change in its representation which will make it impossible to detect two objects that are close in shape.

d. Uniqueness: There should be a one-to-one correspondence between objects and their representations. This requirement is only up to the class induced by criterion **b** above. If this criterion is not satisfied, it will be impossible to distinguish objects of different shapes which have the same representation.

e. Detail: The representation should contain information about the object at varying levels of detail. This is important since features on an object usually exist at different scales. Large-scale features describe the basic structure of the object while small-scale features describe fine detail on the object.

f. Robustness: Any arbitrary initial choices should not change the structure of the representation.

g. Local support: The representation should be computed using local support so that incomplete data only affects the representation locally.

h. Ease of implementation: It is advantageous to use a shape representation technique which is as easy as possible to implement. This will help minimize programming and debugging efforts.

i. Matchability: The representation technique should compute a data structure which lends itself easily to a matching algorithm. Such an algorithm would take two representations as input and return a description of the similarity (or dissimilarity) of the shapes they represent. If this criterion is not satisfied, recognition of an object will not be possible even if its representation has been computed.

Shape representation methods for planar curves previously proposed in computational vision fail to satisfy one or more of the criteria outlined above. The

following is a summary of those methods and the criteria each fails to satisfy:

a. *Hough transform*: Has been used to detect lines [Hough 1962], circles [Duda & Hart 1972] and arbitrary shapes [Ballard 1981]. Edge elements in the image vote for the parameters of the objects of which they are parts. The votes are accumulated in a parameter space. The peaks of the parameter space then indicate the parameters of the objects searched for. For any object more complicated than a line, the parameter space becomes multi-dimensional and therefore the Hough transform fails to satisfy the efficiency criterion. The parameters which define an object change when it undergoes rotation, uniform scaling or translation therefore the invariance criterion is not satisfied either. The local support criterion is also not satisfied since in order to obtain a distinguishable peak in the parameter space, the entire object must be present in the image.

b. *Chain encoding* [Freeman 1974, McKee & Aggarwal 1977] and *polygonal approximations* [Pavlidis 1972, 1977]: The curve is approximated using a polygon or line segments which lie on a grid. These methods do not satisfy the invariance criterion since the approximating polygon rotates, scales and moves as the original curve rotates, scales and moves. Furthermore, the robustness criterion is not satisfied since changing the starting point on the curve can change the shape of the approximating polygon, and the sensitivity criterion is not satisfied since a small change in the shape of the curve can drastically change the shape of the approximating polygon.

c. *Shape factors and quantitative measurements* [Danielsson 1978]: The shape of the object is described using one or more global quantitative measurements of the object such as area, perimeter and compactness. The uniqueness criterion is not satisfied since there is a dramatic reduction in data. The detail criterion is not satisfied since only one scale is represented. Furthermore, the local support criterion is not satisfied since the entire object must be present in the image and the sensitivity criterion is not satisfied since even large changes in the shape of an object may cause no change in its representation.

d. *Strip trees* [Davis 1977, Ballard & Brown 1982]: A strip tree is a set of approximating polygons or polylines ordered such that each polygon or polyline approximates the curve with less approximation error than the previous polygon or polyline. This class also suffers from the shortcomings of class **b.**

e. *Splines* [Ballard & Brown 1982]: The curve is represented using a set of analytic and smooth curves. The invariance criterion is not satisfied since shape-preserving transformations of the curve change the parameters of the

approximating splines. The uniqueness criterion is not satisfied since reconstruction of the original curve is not possible. The robustness criterion is also not satisfied since a particular choice of knot points results in a particular set of approximating splines.

f. *Smoothing splines* [Shahraray & Anderson 1989]: The curve is parametrized to obtain two coordinate functions. Cross-validated regularization [Wahba 1977] is then used to arrive at an "optimal" smoothing of each coordinate function. The smoothed functions together define a new smooth curve. This method does not satisfy the efficiency criterion since cross-validation is quite expensive. It does not satisfy the detail criterion since the object is represented at only one scale. It does not satisfy the uniqueness criterion since the reconstruction of the original curve is not possible, It also does not satisfy the local support criterion since all data points must be present for cross-validation.

g. *Fourier descriptors* [Persoon & Fu 1974]: The curve is represented by the coefficients of the Fourier expansion of a parametric representation of the curve. The invariance criterion is not satisfied by this class since shape-preserving transformations of the curve will change its Fourier coefficients. The local support criterion is also not satisfied since the entire curve must be available in order to compute its Fourier expansion.

h. *Curvature primal sketch* [Asada & Brady 1984]: The curve is approximated using a library of well-defined, analytic curves. Then the curvature function of the approximating curve is computed and convolved with a Gaussian of varying standard deviation. This method does not satisfy the sensitivity criterion. If the original curve is noisy, then computing its curvature function is an error-prone process and the computed representation may change significantly. More will be said on this method in section 6.

i. *Extended circular image* [Horn & Weldon 1986]: This representation is the two-dimensional equivalent of the *extended Gaussian image*. In the extended circular image, one is given the radius of curvature as a function of normal direction. The invariance criterion is not satisfied by this method since the representation rotates as the original curve rotates. The uniqueness criterion is also not satisfied since the representation is one-to-one only for the class of simple and convex curves.

j. *Volumometric diffusion* [Koenderink & van Doorn 1986]: A geometrical object is defined by way of its "characteristic function" $\chi(\mathbf{r})$ which equals unity when the point $\mathbf{r}$ belongs to the object and zero otherwise. The object is then blurred by requiring that its characteristic function satisfy the diffusion

equation. The boundary of each blurred object is defined by the equation $\chi(\mathbf{r}) = 0.5$. The efficiency criterion is not satisfied by this method since an image must be convolved with a large number of two-dimensional Gaussian filters. The invariance criterion is also not satisfied since shape-preserving transformations of the object also change the blurred objects computed by this method.

A multi-scale representation for one-dimensional functions was first proposed by Stansfield [1980] and later developed by Witkin [1983]. The function $f(x)$ is convolved with a Gaussian function as its variance σ^2 varies from a small to a large value. The zero-crossings of the second derivative of each convolved function are extracted and marked in the x–σ plane. The result is the *scale space image* of the function.

The *curvature scale space image* was introduced in [Mokhtarian & Mackworth 1986] as a new shape representation for planar curves. The representation is computed by convolving a path-based parametric representation of the curve with a Gaussian function, as the standard deviation of the Gaussian varies from a small to a large value, and extracting the curvature zero-crossing points of the resulting curves. The representation is essentially invariant under rotation, uniform scaling and translation of the curve. This and a number of other properties makes it suitable for recognizing a noisy curve of arbitrary shape at any scale or orientation. The process of describing a curve at increasing levels of abstraction is referred to as the *evolution* of that curve. The evolution of a planar curve and the curvature scale space image are described in detail in section **2**.

Mackworth and Mokhtarian [1988] introduced a modification of the curvature scale space image referred to as the *renormalized curvature scale space image*. This representation is computed in a similar fashion but the curve is reparametrized by arc length after convolution. As was demonstrated in [Mackworth & Mokhtarian 1988], the renormalized curvature scale space image is more suitable for recognizing a curve with non-uniform noise added to it. However, unlike the regular curvature scale space representation, the renormalized curvature scale space applies only to closed curves. The renormalized curvature scale space image is described in detail in section **3**.

The *resampled curvature scale space image* is a substantial refinement of the curvature scale space which is based on the concept of *arc length evolution*. It is shown that the resampled curvature scale space image is more suitable than the renormalized curvature scale space image for recognition of curves with added non-uniform noise or when local shape differences exist. The arc length evolution of a planar curve and the resampled curvature scale space image are described in detail in section **4**.

Section **5** contains descriptions of the evolution and arc length evolution properties of planar curves. Almost all these properties are shown to be true of both evolution and arc length evolution. Together, these properties provide a theoretical foundation for the representation method proposed in this paper. The proofs of the lemmas and theorems of section **5** are given in the appendix.

Section **6** discusses the significance of the evolution and arc length evolution properties described in section **5**. It argues that these properties show that:

a. Evolution and arc length evolution are physically plausible operations.

b. There exist strong constraints on the location of a planar curve during evolution or arc length evolution.

c. The representations based on evolution and arc length evolution satisfy almost all of the criteria required of any shape representation method.

d. Behaviour of a planar curve during evolution or arc length evolution can be completely characterized. For example, the shape of a planar curve can be locally determined before and after the creation of a cusp point. This behaviour corresponds to a "natural" multi-scale desription of the curve.

Section **7** presents the conclusions of this paper.

2. The curvature scale space image

A planar curve is a set of points whose position vectors are the values of a continuous vector-valued and locally one-to-one function. It can be represented by the parametric vector equation

$$\mathbf{r}(u) = (x(u), y(u)) \tag{2.1}$$

The function $\mathbf{r}(u)$ is a parametric representation of the curve. A planar curve has an infinite number of distinct parametric representations. A parametric representation in which the parameter is the arc length s is called a *natural* parametrization of the curve. A natural parametrization can be computed from an arbitrary parametrization using the following equation

$$s = \int_0^u |\dot{\mathbf{r}}(v)|\, dv.$$

For any parametrization

$$\dot{\mathbf{r}}(u) = (\dot{x}(u), \dot{y}(u))$$

$$|\dot{\mathbf{r}}(u)| = (\dot{x}^2 + \dot{y}^2)^{1/2}$$

$$\mathbf{t}(u) = \frac{\dot{\mathbf{r}}}{|\dot{\mathbf{r}}|} = \Big(\frac{\dot{x}}{(\dot{x}^2 + \dot{y}^2)^{1/2}}, \frac{\dot{y}}{(\dot{x}^2 + \dot{y}^2)^{1/2}} \Big)$$

$$\mathbf{n}(u) = \Big(\frac{-\dot{y}}{(\dot{x}^2 + \dot{y}^2)^{1/2}}, \frac{\dot{x}}{(\dot{x}^2 + \dot{y}^2)^{1/2}} \Big)$$

where $\mathbf{t}(u)$ and $\mathbf{n}(u)$ are the tangent and normal vectors at u respectively.

For any planar curve the vectors $\mathbf{t}(u)$ and $\mathbf{n}(u)$ must satisfy the simplified Serret-Frenet vector equations [Goetz 1970]:

$$\mathbf{t}'(s) = \kappa(s)\,\mathbf{n}(s)$$

$$\mathbf{n}'(s) = -\kappa(s)\,\mathbf{t}(s)$$

where $\kappa(s)$ is the curvature of the curve at s and is defined to be the inverse of the radius of the osculating circle at s. The osculating circle at s has a higher degree of contact with the curve at s than any other circle. Now observe that:

$$\mathbf{t}'(s) = \frac{d\mathbf{t}}{ds} = \frac{d\mathbf{t}}{du}\frac{du}{ds}.$$

Therefore

$$\frac{d\mathbf{t}}{du} = \frac{ds}{du}\,\kappa\,\mathbf{n} = |\dot{\mathbf{r}}|\,\kappa\,\mathbf{n}.$$

Hence

$$\kappa(u) = \frac{\dot{\mathbf{t}}\,.\,\mathbf{n}}{|\dot{\mathbf{r}}|}.$$

Differentiating the expression for $\mathbf{t}(u)$, we obtain:

$$\dot{\mathbf{t}}(u) = \Big(\frac{-\dot{y}(\dot{x}\dddot{y} - \dddot{x}\dot{y})}{(\dot{x}^2 + \dot{y}^2)^{3/2}}, \frac{\dot{x}(\dot{x}\dddot{y} - \dddot{x}\dot{y})}{(\dot{x}^2 + \dot{y}^2)^{3/2}} \Big).$$

It now follows that:

$$\kappa(u) = \frac{\dot{x}(u)\ddot{y}(u) - \dot{y}(u)\ddot{x}(u)}{(\dot{x}(u)^2 + \dot{y}(u)^2)^{3/2}}.$$

Therefore it is possible to compute the curvature of a planar curve from its parametric representation.

Two special cases of the parametrization, of interest here, yield simplifications of these formulas. If we have a natural path representation with s, the arc length parameter, ranging over $[0, L]$ then:

$$|\,\dot{\mathbf{r}}(s)\,| = |\,(\dot{x}(s),\,\dot{y}(s))\,| = (\dot{x}^2(s) + \dot{y}^2(s))^{1/2} = 1$$

$$\mathbf{t}(s) = (\dot{x}(s),\ \dot{y}(s))$$

$$\dot{\mathbf{t}}(s) = (\ddot{x}(s),\ \ddot{y}(s))$$

$$\mathbf{n}(s) = (-\dot{y}(s),\ \dot{x}(s))$$

$$k(s) = \dot{\mathbf{t}}(s)\cdot\mathbf{n}(s)$$

and

$$k(s) = \dot{x}(s)\ddot{y}(s) - \ddot{x}(s)\dot{y}(s).$$

Note also

$$k^2(s) = |\dot{\mathbf{t}}(s)|^2$$

$$k^2(s) = \ddot{x}^2(s)+\ddot{y}^2(s).$$

If the parameter is a linear rescaling of the arc length ranging over [0,1], the normalized path length parameter w, then

$$w = \frac{s}{L}$$

$$|\dot{\mathbf{r}}(w)| = L$$

$$\mathbf{t}(w) = \frac{1}{L}(\dot{x}(w),\ \dot{y}(w))$$

$$\mathbf{n}(w) = \frac{1}{L}(-\dot{y}(w),\ \dot{x}(w))$$

$$k(w) = \frac{1}{L^3}(\dot{x}(w)\ddot{y}(w)-\ddot{x}(w)\dot{y}(w))$$

and

$$k^2(w) = \frac{1}{L^4}(\ddot{x}^2(w)+\ddot{y}^2(w)).$$

Given a planar curve

$$\Gamma = \{(x(w), y(w))|w \in [0,1]\}$$

where w is the normalized arc length parameter, an *evolved* version of that curve is defined by

$$\Gamma_\sigma = \{(X(u,\sigma),\ Y(u,\sigma))|u \in [0,1]\}$$

where

$$X(u,\sigma) = x(u) \circledast g(u,\sigma)$$

$$Y(u,\sigma) = y(u) \circledast g(u,\sigma)$$

Function $g(u,\sigma)$ denotes a Gaussian of width σ [Marr & Hildreth 1980] and is defined by

$$g(u,\sigma) = \frac{1}{\sigma\sqrt{2\pi}} e^{\frac{-u^2}{2\sigma^2}}.$$

Functions $X(u,\sigma)$ and $Y(u,\sigma)$ are given explicitly by

$$X(u,\sigma) = \int_{-\infty}^{\infty} x(v) \frac{1}{\sigma\sqrt{2\pi}} e^{\frac{-(u-v)^2}{2\sigma^2}} dv$$

and

$$Y(u,\sigma) = \int_{-\infty}^{\infty} y(v) \frac{1}{\sigma\sqrt{2\pi}} e^{\frac{-(u-v)^2}{2\sigma^2}} dv.$$

The curvature of Γ_σ is given by

$$\kappa(u,\sigma) = \frac{X_u(u,\sigma)\, Y_{uu}(u,\sigma) - X_{uu}(u,\sigma)\, Y_u(u,\sigma)}{(X_u(u,\sigma)^2 + Y_u(u,\sigma)^2)^{3/2}}$$

where

$$X_u(u,\sigma) = \frac{\partial}{\partial u}(x(u) \circledast g(u,\sigma)) = x(u) \circledast g_u(u,\sigma)$$

$$X_{uu}(u,\sigma) = \frac{\partial^2}{\partial u^2}(x(u) \circledast g(u,\sigma)) = x(u) \circledast g_{uu}(u,\sigma)$$

$$Y_u(u,\sigma) = y(u) \circledast g_u(u,\sigma)$$

and

$$Y_{uu}(u,\sigma) = y(u) \circledast g_{uu}(u,\sigma).$$

The process of generating the ordered sequence of curves $\{\Gamma_\sigma | \sigma \geq 0\}$ is referred to as the *evolution* of Γ.

Figure 2.1 shows a planar curve depicting the shoreline of Africa. Figure 2.2 shows several evolved versions of that curve for increasing values of σ. Note that when a planar curve evolves according to the process defined above, its total arc length shrinks. The amount of shrinkage is directly proportional to the value of σ. In certain applications, this may be an undesirable feature. For example, the evolution process defined above may be used to smooth edges extracted from an image by an edge detector. However, it may be advantageous to have the smoothed edges at the same physical location as the original edges. This can be accomplished by estimating the amount of movement at each point on the

smoothed edges and adding a vector to the location vector of that point to compensate for that movement [Lowe 1988]. The result is a smoothed curve which is physically close to the original curve.

The function defined implicitly by

$$\kappa(u,\sigma) = 0$$

is the *curvature scale space image* of Γ [Mokhtarian & Mackworth 1986]. Figure 2.3 shows the curvature scale space of the curve of figure 2.1. Figure 2.4 shows Koch's snowflake curve and several of its evolved versions. Figure 2.5 shows the curvature scale space image of the snowflake curve. Figure 2.6 shows a design from a Persian carpet and several evolved versions. Figure 2.7 shows the curvature scale space image of that design.

3. The renormalized curvature scale space image

Mackworth and Mokhtarian [1988] observed that although w is the normalized arc length parameter on the original curve Γ, the parameter u is **not**, in general, the normalized arc length parameter on the evolved curve Γ_σ. Figure 3.1 shows the shoreline of Africa with noise added to its lower half. Figure 3.2 shows the curvature scale space of that curve. A comparison of figures 2.3 and 3.2 shows that there does not exist a good match of one curvature scale space image to the other. To overcome this problem, Mackworth and Mokhtarian [1988] proposed the *renormalized* curvature scale space image.

Let

$$\mathbf{R}(u,\sigma) = (X(u,\sigma), Y(u,\sigma))$$

and

$$w = \Phi_\sigma(u)$$

where

$$\Phi_\sigma(u) = \frac{\int_0^u |\mathbf{R}_v(v,\sigma)|\,dv}{\int_0^1 |\mathbf{R}_v(v,\sigma)|\,dv}.$$

Now define

$$\hat{X}(w,\sigma) = X(\Phi_\sigma^{-1}(w),\sigma) \qquad \hat{Y}(w,\sigma) = Y(\Phi_\sigma^{-1}(w),\sigma). \tag{3.1}$$

That is, each evolved curve Γ_σ is reparametrized by its normalized arc length parameter w.

Notice that

$$\Phi_\sigma(0) = 0$$

$$\Phi_\sigma(1) = 1$$

and

$$\frac{d\Phi_\sigma(u)}{du} = \frac{|\mathbf{R}_u(u,\sigma)|}{\int_0^1 |\mathbf{R}_v(v,\sigma)|\,dv} > 0 \qquad \text{at non-singular points.}$$

Also

$$\Phi_0(u) = u.$$

$\Phi_\sigma(u)$ deviates from the identity function $\Phi_\sigma(u) = u$ only to the extent to which the scale-related satistics deviate from stationarity along the original curve.

Once we have changed parameters according to equations (3.1), the curvature of the curve with the normalized path length parameter is given by

$$\kappa(w,\sigma) = \frac{1}{L^3}[\hat{X}_w(w,\sigma)\,\hat{Y}_{ww}(w,\sigma) - \hat{X}_{ww}(w,\sigma)\,\hat{Y}_w(w,\sigma)].$$

The function defined implicitly by

$$\kappa(w,\sigma) = 0$$

is the *renormalized* curvature scale space image of Γ. Figure 3.3 shows the renormalized curvature scale space of Africa and figure 3.4 shows the renormalized curvature scale space of noisy Africa. It can be seen that the degree of match of figure 3.3 to figure 3.4 is much better than the degree of match of figure 2.3 to figure 3.2.

4. The resampled curvature scale space image

Note that as a planar curve evolves according to the process defined in section **2**, the parametrization of its coordinate functions $x(u)$ and $y(u)$ does not change. In other words, the function mapping values of the parameter u of the original coordinate functions $x(u)$ and $y(u)$ to the values of the parameter u of the smoothed coordinate functions $X(u,\sigma)$ and $Y(u,\sigma)$ is the identity function.

For both theoretical and practical reasons, it is interesting to generalize the definition of evolution so that the mapping function can be different from the identity function. Again let Γ be defined by:

$$\Gamma = \{(x(w), y(w)) | w \in [0,1]\}.$$

The generalized evolution which maps Γ to Γ_σ is now defined by:

$$\Gamma \longrightarrow \Gamma_\sigma = \{(X(W,\sigma), Y(W,\sigma)) | W \in [0,1]\}$$

where

$$X(W,\sigma) = x(W) \circledast g(W,\sigma)$$

and

$$Y(W,\sigma) = y(W) \circledast g(W,\sigma).$$

Note that

$$W = W(w,\sigma)$$

and

$$W(w,\sigma_0)$$

where σ_0 is any value of σ, is a continuous and monotonic function of w. This condition is necessary to ensure physical plausibility since W is the parameter of the evolved curve Γ_σ.

A specially interesting case is when W always remains the arc length parameter as the curve evolves. When this criterion is satisfied, the evolution of Γ is refered to as *arc length evolution*. An explicit formula for W can be derived [Gage & Hamilton 1986].

Recall equation (2.1)

$$\mathbf{r}(u) = (x(u), y(u)).$$

The Frenet equations for a planar curve are given by

$$\frac{\partial \mathbf{t}}{\partial u} = |\frac{\partial \mathbf{r}}{\partial u}| \kappa \mathbf{n}$$

$$\frac{\partial \mathbf{n}}{\partial u} = -|\frac{\partial \mathbf{r}}{\partial u}| \kappa \mathbf{t}.$$

Let $t = \sigma^2/2$. Observe that

$$\frac{\partial}{\partial t}(|\frac{\partial \mathbf{r}}{\partial u}|^2) = \frac{\partial}{\partial t}(\frac{\partial \mathbf{r}}{\partial u} \cdot \frac{\partial \mathbf{r}}{\partial u}) = 2(\frac{\partial \mathbf{r}}{\partial u} \cdot \frac{\partial^2 \mathbf{r}}{\partial u \partial t}).$$

Note that

$$\frac{\partial \mathbf{r}}{\partial u} = |\frac{\partial \mathbf{r}}{\partial u}| \mathbf{t}$$

and

$$\frac{\partial \mathbf{r}}{\partial t} = \kappa \mathbf{n}$$

since the Gaussian function satisfies the heat equation. It follows that

$$\frac{\partial}{\partial t}(|\frac{\partial \mathbf{r}}{\partial u}|^2) = 2(|\frac{\partial \mathbf{r}}{\partial u}|\,\mathbf{t}\,.\frac{\partial}{\partial u}(\kappa\,\mathbf{n})) = 2(|\frac{\partial \mathbf{r}}{\partial u}|\,\mathbf{t}\,.(\frac{\partial \kappa}{\partial u}\,\mathbf{n} - |\frac{\partial \mathbf{r}}{\partial u}|\,\kappa^2\,\mathbf{t})) = -2|\frac{\partial \mathbf{r}}{\partial u}|^2\,\kappa^2.$$

Therefore

$$2|\frac{\partial \mathbf{r}}{\partial u}|\;\frac{\partial}{\partial t}|\frac{\partial \mathbf{r}}{\partial u}| = -2\,|\frac{\partial \mathbf{r}}{\partial u}|^2\,\kappa^2$$

or

$$\frac{\partial}{\partial t}|\frac{\partial \mathbf{r}}{\partial u}| = -|\frac{\partial \mathbf{r}}{\partial u}|\,\kappa^2.$$

Let L denote the length of the curve. Now observe that

$$\frac{\partial L}{\partial t} = \int_0^L \frac{\partial}{\partial t}|\frac{\partial \mathbf{r}}{\partial u}|\,du = -\int_0^L |\frac{\partial \mathbf{r}}{\partial u}|\,\kappa^2\,du = -\int_0^1 \kappa^2\,dw.$$

Since the value w_0 of the normalized arc length parameter w at a point P measures the length of the curve from the starting point to point P, it follows that

$$\frac{\partial W}{\partial t} = -\int_0^W \kappa^2(W,t)\,dW$$

and therefore

$$W(w,t) = -\int_0^t \int_0^W \kappa^2(W,t)\,dW\,dt. \tag{4.1}$$

Note that

$$W(w,0) = w.$$

The function defined implicitly by

$$\kappa(W,\sigma) = 0$$

is the *resampled* curvature scale space of Γ.

Since the function $\kappa(W,t)$ in (4.1) is unknown, $W(w,t)$ can not be computed directly from (4.1). However, the resampled curvature scale space can be computed in a simple way. A Gaussian filter based on a small value of the standard deviation is computed. The curve Γ is parametrized by the normalized arc length parameter and convolved with the filter. The resulting curve is reparametrized by the normalized arc length parameter and convolved again with the same filter. This process is repeated until the curve is convex and no longer has any curvature zero-crossing points. The curvature zero-crossings of each curve are marked in the resampled curvature scale space image. Note that the standard deviation of the Gaussian chosen above should be small enough so that the deviation from arc length parametrization after each iteration is negligible. Then the entire process can be considered to model arc length evolution.

Figure 4.1 shows the resampled curvature scale space of Africa and figure 4.2 shows the resampled curvature scale space of noisy Africa. Note that a very close match can be observed when matching figure 4.1 to figure 4.2. However, it should be noted that the regular and renormalized curvature scale space images of a planar curve have exactly the same number of rows and columns *but* its resampled curvature scale space image, in general, differs in the number of rows. This property suggests that matching a renormalized curvature scale space image to a regular curvature scale space image may be easier than matching a resampled curvature scale space image to a renormalized or regular curvature scale space image.

5. Evolution and arc length evolution properties of planar curves

This section contains a number of important results on evolution and arc length evolution of planar curves as defined in sections 2 and 4. Unless otherwise stated, the proofs in appendix are given only for arc length evolution. The proofs for regular evolution are similar and simpler.

The first five lemmas express a number of fundamental properties of evolution and arc length evolution.

Lemma 1. Evolution and arc length evolution of a planar curve are invariant under the shape preserving transformations (rotation, uniform scaling and translation) of the curve.

Lemma 2. A closed planar curve remains closed during its evolution and arc length evolution.

Lemma 3. A connected planar curve remains connected during its evolution and arc length evolution.

Lemma 4. The center of mass of a planar curve does not move during evolution and arc length evolution of that curve.

Lemma 5. Let Γ be a closed planar curve and let G be its convex hull. Γ remains inside G during evolution and arc length evolution.

Theorem 1 shows that the mapping from a planar curve to its curvature scale space image is an invertible one.

Theorem 1. Let Γ be a planar curve in C_1. A single point on one curvature zero-crossing contour in the regular, renormalized or resampled curvature scale space image of Γ determines Γ uniquely up to uniform scaling, rotation and

translation (except on a set of measure zero).

Theorem 2 states that under certain conditions, new curvature zero-crossing points are not created during evolution and arc length evolution of planar curves.

Theorem 2. Let Γ be a planar curve in C_2. If all evolved and arc length evolved curves Γ_σ are in C_2, then all extrema of contours in the regular, renormalized and resampled curvature scale space images of Γ are maxima.

Theorem 3 locally characterizes the behaviour of planar curves during evolution and arc length evolution just before the creation of a cusp point.

Theorem 3. Let $\Gamma = (x(u),y(u))$ be a planar curve in C_1 and let $x(u)$ and $y(u)$ be polynomial functions of u. Let Γ_σ be an evolved or arc length evolved version of Γ with a cusp point at u_0. There is a $\delta>0$ such that $\Gamma_{\sigma-\delta}$ intersects itself in a neighborhood of point u_0.

The following theorem holds only for arc length evolution.

Theorem 4. Simple curves remain simple during arc length evolution.

Theorem 5 locally characterizes the behaviour of a planar curve during evolution and arc length evolution just after the creation of a cusp point.

Theorem 5: Let $\Gamma = (x(u), y(u))$ be a planar curve in C_1 and let $x(u)$ and $y(u)$ be polynomial functions of u. Let Γ_σ be an evolved version of Γ with a cusp point at u_0. There is a $\delta>0$ such that $\Gamma_{\sigma+\delta}$ has two new curvature zero-crossings in a neighborhood of u_0.

6. Discussion

Three different multi-scale representation techniques for planar curves were described in this paper. These three are: the regular curvature scale space image, the renormalized curvature scale space image and the resampled curvature scale space image. Each representation technique is suitable for specific applications. When little or no noise exists on the curve, the regular curvature scale space image can be used. However, when there is non-uniform noise on the curve or when there are local shape differences between the model curves and the image curves, either the renormalized or the resampled curvature scale space images should be used. The renormalized curvature scale space image is the most computationally intensive and it can not be computed for open curves but it has the advantage that it has the same number of rows and columns as the regular curvature scale space image for the same curve. Observations indicate that when there are local shape differences, the resampled curvature scale space images show

the best overall match whereas the renormalized curvature scale space images match well at high scales but are more influenced by the shape differences at lower scales. Therefore the choice of the representation technique should depend on the scale level of the curve features that one wishes to emphasize. Table 1 summarizes the advantages and disadvantages of each representation technique:

Representation technique	Advantages	Disadvantages
The Regular Curvature Scale Space Image	• Suitable for transformations consisting of uniform scaling, rotation and translation. • Suitable when uniform, low-intensity noise has corrupted the curve.	• Non-uniform noise or local difference in shape can cause problems.
The Renormalized Curvature Scale Space Image	• More suitable when there is non-uniform noise on the curve or local shape differences exist. • Has the same number of rows and columns as the regular CSSI.	• Most computationally intensive. • Can not be computed for open curves.
The Resampled Curvature Scale Space Image	• Most suitable when there is high-intensity, non-uniform noise or local shape differences exist. • Can also be computed for open curves.	• The number of rows is in general different from number of rows of regular and renormalized curvature scale space images.

Table 1. Comparison of Regular, Renormalized and Resampled Curvature Scale Space Images.

The following is a discussion of the practical significance of the lemmas and theorems of section 5.

Lemma 1 showed that evolution and arc length evolution of a planar curve are invariant under rotation, uniform scaling and translation of the curve. This shows that the regular, renormalized and resampled curvature scale space images of a planar curve have the *invariance* property [Mokhtarian & Mackworth 1986]. The invariance property is essential since it makes it possible to match a planar curve to another of similar shape which has undergone a transformation consisting of arbitrary amounts of rotation, uniform scaling and translation.

Lemmas **2** and **3** showed that connectedness and closedness of a planar curve are preserved during evolution and arc length evolution. These lemmas show that evolution and arc length evolution of a planar curve are physically plausible operations. Consider a closed, connected planar curve that represents the boundary of a two-dimensional object. If such a curve is not closed or connected after evolution or arc length evolution, then it can no longer admit a physically plausible interpretation.

Lemma **4** showed that the center of mass of a planar curve does not move as the curve evolves and lemma **5** showed that a planar curve remains inside its convex hull during evolution and arc length evolution. Together, lemmas **4** and **5** impose constraints on the physical location of a planar curve as it evolves. These constraints become useful whenever the physical location of curves in an image or their locations with respect to each other is important. A possible application area is stereo matching in which it is advantageous to carry out matching at coarser levels of detail first and then match at fine detail levels to increase accuracy.

Theorem **1** showed that the curvature scale space images of a planar curve determines that curve uniquely modulo uniform scaling, rotation and translation. This shows that the curvature scale space images satisfy the *uniqueness* property [Mokhtarian & Mackworth 1986]. This property ensures that curves of different shapes do not have the same representation.

Theorems **3** and **5** together locally characterize the behaviour of a planar curve just before and just after the formation of a cusp point during evolution and arc length evolution. This behaviour can be used to detect any cusp points that form during evolution or arc length evolution of a planar curve. Such cusp points can then be used effectively to facilitate matching since they provide us with a set of distinctive and easily recognizable features. These theorems also show that self-intersecting curves are described in a natural way by our representation technique. The self-intersection loop gradually grows smaller until it turns into a cusp point and vanishes. In contrast, Asada and Brady's method [1986] enlarges the smaller loop until it becomes as large as the larger loop. Figures 6.1 and 6.2 show two self-intersecting curves during evolution. The self-intersection is resolved through the formation of a cusp point after which the curve becomes simple.

Theorem **2** showed that if a planar curve remains smooth during evolution or arc length evolution, then no new curvature zero-crossings will be observed in its curvature scale space images. Theorem **3** showed that every planar curve intersects itself during evolution or arc length evolution just before the formation of a cusp point and theorem **4** showed that simple curves remain simple during arc length evolution. Combining theorems **2**, **3** and **4**, we conclude that no new

curvature zero-crossing points are created during arc length evolution of simple curves. This is an important result since it indicates that new "structure" is not created in the curvature scale space representations of simple curves [Marr & Nishihara 1978]. Note that a subclass of self-crossing curves also shares this property.

The result stated by theorem 4 is also very important. Simple planar curves usually represent the boundaries of two-dimensional objects. Arc length evolved versions of those curves can only have physical plausibility if they are also simple. Theorem 4 shows that this is in fact the case. Figure 6.3 shows a simple curve and its evolved versions It can be seen that the curve intersects itself during evolution. Figure 6.4 shows the same curve and its arc length evolved versions. As expected, the curve remains simple during arc length evolution.

We now present an evaluation of the curvature scale space representations according to the criteria proposed in section 1.

Criterion a: *Efficiency*

The computation of the representations proposed here calls for evaluation of a large number of convolutions. This process can be rendered efficient using one or more of the following techniques:

i. Fast Fourier transforms
ii. Parallelism
iii. Expression of convolutions involving Gaussians of large widths in terms of convolutions involving Gaussians of small widths only
iv. Tracking the curvature zero-crossing points across multiple scales. When it is known that new curvature zero-crossings will not be created at higher scales, convolutions can be carried out only in a small neighborhood of the existing zero-crossings in order to find the zero-crossings at the next higher level.

Furthermore, curvature scale space representations can be stored very efficiently as binary images.

Criterion b: *Invariance*

Translation of the curve causes no change in the curvature scale space representations proposed here. Rotation causes only a horizontal shift in the curvature scale space representations and uniform scaling causes the curvature scale space representations to undergo uniform scaling as well. If the represented curves are closed, then their curvature scale space representations can be normalized and invariance with respect to uniform scaling will also be achieved. If the represented curves are open, changes due to uniform scaling can be handled by the matching algorithm.

Criterion c: *Sensitivity*

Small changes to the shape of the curve almost always result in small changes in its representation since smaller values of the scale parameter will be sufficient to smooth out the change.

Criterion d: *Uniqueness*

As argued earlier, theorem **1** shows that a planar curve can be reconstructed from any of its curvature scale space representations and therefore the curvature scale space representations satisfy the uniqueness criterion.

Criterion e: *Detail*

Since the curvature scale space representations combine information about the curve at varying levels of detail, criterion **e** is also satisfied.

Criterion f: *Robustness*

The only arbitrary choice to be made when computing the curvature scale space representations is the starting point for parametrization on a closed curve. This only causes a horizontal shift in the curvature scale space representations but it causes no structural change.

Criterion g: *Local support*

All convolutions are carried out using finite Gaussian filters therefore criterion **g** is also satisfied.

Criterion h: *Ease of implementation*

The procedures needed to compute the curvature scale space image are quite easy and straightforward to implement. All that is needed is to prepare masks approximating derivatives of Gaussians and to convolve those with the coordinate functions of the input curve. Curvature zero-crossings are then readily located and their locations stored in a two-dimensional array. Hence criterion **h** is also satisfied.

Criterion i: *Matchability*

A curvature scale space image consists of curvature zero-crossing contours which can be matched in a straightforward way to contours in other curvature scale space images. For a curvature scale space matching algorithm, see [Mokhtarian & Mackworth 1986].

It follows that the curvature scale space representations satisfy the necessary criteria for shape representation methods better than shape representation techniques previously proposed.

7. Conclusions

This paper introduced a novel shape representation technique for planar curves and proposed a number of necessary criteria that any useful shape representation scheme should satisfy. Those criteria are: efficiency, invariance, sensitivity, uniqueness, detail, robustness, local support, ease of implementation and matchability.

Three different ways of computing the representation were described. Each method relies on extracting features of the curve that are invariant under shape preserving transformations at varying scales. These methods result in: the curvature scale space image, the renormalized curvature scale space image and the resampled curvature scale space image. It was shown that each of those representations is suitable for a specific application.

A number of theoretical properties of those representations were also investigated. These properties together provide a sound foundation for the representations proposed in this paper. Finally, it was shown that the proposed representations satisfy the criteria introduced earlier better than previously proposed shape representation techniques for planar curves.

Acknowledgments

We wish to thank David Lowe and Jim Little for their helpful comments. This work was supported by the Natural Sciences and Engineering Research Council of Canada, the Canadian Institute for Advanced Research and the University of British Columbia.

References

Asada, H. and M. Brady, "The curvature primal sketch," *IEEE PAMI*, vol. 8, pp. 2-14, 1986.

Ballard, D. H., "Generalizing the Hough transform to detect arbitrary shapes," *Pattern Recognition*, vol. 13, pp. 111-122, 1981.

Ballard, D. H. and C. M. Brown, *Computer Vision*, Prentice-Hall, Englewood Cliffs, NJ, 1982.

Danielsson, P. E., "A new shape factor," *CGIP*, vol. 7, pp. 292-299, 1978.

Davis, L. S., "Understanding shape: Angles and sides," *IEEE Trans. Computers*, vol. C-26, pp. 236-242, 1977.

Duda, R. O. and P. E. Hart, "Use of the Hough transformation to detect lines and curves in pictures," *Comm. ACM*, vol. 15, pp. 11-15, 1972.

Freeman, H., "Computer processing of line-drawing images," *Comput. Surveys*, vol. 6, 1974.

Gage, M. and R. S. Hamilton, "The heat equation shrinking convex plane curves," *J. Differential Geometry*, vol. 23, pp. 69-96, 1986.

Goetz, A., *Introduction to differential geometry*, Addison Wesley, Reading, MA, 1970.

Haralick, R. M., A. K. Mackworth, and S. L. Tanimoto, "Computer vision update," Technical report 89-12, Dept. Computer Science, University of British Columbia, Vancouver, B.C., 1989.

Horn, B. K. P. and E. J. Weldon, "Filtering closed curves," *IEEE PAMI*, vol. 8, pp. 665-668, 1986.

Hough, P. V. C., "Method and means for recognizing complex patterns," U.S. patent 3 069 654, 1962.

Hummel, R. A., B. Kimia, and S. W. Zucker, "Deblurring Gaussian blur," *CVGIP*, vol. 38, pp. 66-80, 1987.

Kecs, W., *The convolution product and some applications*, D. Reidel, Boston, MA, 1982.

Lowe, D., "Organization of smooth image curves at multiple scales," *Proc. ICCV*, pp. 558-567, Tampa, Florida, 1988.

Mackworth, A. K. and F. Mokhtarian, "The renormalized curvature scale space and the evolution properties of planar curves," *Proc. IEEE CVPR*, pp. 318-326, Ann Arbor, Michigan, 1988.

McKee, J. W. and J. K. Aggarwal, "Computer recognition of partial views of curved objects," *IEEE Trans. Computers*, vol. C-26, pp. 790-800, 1977.

Mokhtarian, F. and A. K. Mackworth, "Scale-based description and recognition of planar curves and two-dimensional shapes," *IEEE PAMI*, vol. 8, pp. 34-43, 1986.

Mokhtarian, F., "Fingerprint theorems for curvature and torsion zero-crossings," *Proc. IEEE CVPR*, pp. 269-275, San Diego, California, 1989.

Pavlidis, T., "Segmentation of pictures and maps through functional approximations," *CGIP*, vol. 1, pp. 360-372, 1972.

Pavlidis, T., "Polygonal approximations by Newton's method," *IEEE Trans. Computers*, vol. C-26, pp. 800-807, 1977.

Persoon, E. and K. S. Fu, "Shape discrimination using Fourier descriptors," *Proc. IJCPR*, pp. 126-130, Copenhagen, Denmark, 1974.

Saund, E., "Adding scale to the primal sketch," *Proc. IEEE CVPR*, pp. 70-78, San Diego, California, 1989.

Shahraray, B. and D. J. Anderson, "Optimal estimation of contour properties by cross-validated regularization," *IEEE PAMI*, vol. 11, pp. 600-610, 1989.

Stansfield, J. L., "Conclusions from the commodity expert project," AI memo 601, MIT AI Lab, Cambridge, MA, 1980.

Wahba, G., "A survey of some smoothing problems and the method of generalized cross-validation for solving them," in *Applications of Statistics*, P. R. Krishnaiah, Ed., Amsterdam, The Netherlands: North-Holland, 1977.

Witkin, A. P., "Scale space filtering," *Proc. IJCAI*, pp. 1019-1023, Karlsruhe, W. Germany, 1983.

Yuille, A. L. and T. A. Poggio, "Scaling theorems for zero-crossings," *IEEE PAMI*, vol. 8, pp. 15-25, 1986.

Appendix

Proof of lemma 1: It will be shown that arc length evolution is invariant under a general affine transform. Let $\Gamma_\sigma = (X(W,\sigma), Y(W,\sigma))$ be an arc length evolved version of $\Gamma = (x(w),y(w))$. If Γ_σ is transformed according to an affine transform, then at its new coordinates, X_1 and Y_1, are given by

$$X_1(W,\sigma) = a\,X(W,\sigma) + b\,Y(W,\sigma) + c$$

$$Y_1(W,\sigma) = d\,X(W,\sigma) + e\,Y(W,\sigma) + f.$$

Now suppose Γ is transformed according to an affine transform and then evolved. The coordinates X_2 and Y_2 of the new curve are

$$X_2(W,\sigma) = (a\,x(W) + b\,y(W) + c) \circledast g(W,\sigma)$$

$$Y_2(W,\sigma) = (d\,x(W) + e\,y(W) + f) \circledast g(W,\sigma).$$

Since the convolution operator is distributive [Kecs 1982], it follows that

$$X_2(W,\sigma) = X_1(W,\sigma)$$

$$Y_2(W,\sigma) = Y_1(W,\sigma)$$

and the lemma follows. □

Proof of lemma 2: Let $\Gamma = (x(w),y(w))$ be a closed curve and let $\Gamma_\sigma = (X(W,\sigma), Y(W,\sigma)$ be an arc length evolved version of Γ. On Γ:

$$(x(0), y(0)) = (x(1), y(1)).$$

On Γ_σ:

$$(X(0,\sigma), Y(0,\sigma)) = (X(1,\sigma), Y(1,\sigma)).$$

It follows that Γ_σ is closed. □

Proof of lemma 3: Let $\Gamma = (x(w),y(w))$ be a connected planar curve and $\Gamma_\sigma = (X(W,\sigma), Y(W,\sigma))$ be an arc length evolved version of that curve. Since Γ is connected, $x(w)$ and $y(w)$ are continuous functions and therefore $X(W,\sigma)$ and $Y(W,\sigma)$ are also continuous. Let W_0 be any value of parameter W and let x_0 and y_0 be the values of $X(W,\sigma)$ and $Y(W,\sigma)$ at W_0 respectively. If W goes through an infinitesimal change, then $X(W,\sigma)$ and $Y(W,\sigma)$ will also go through infinitesimal changes:

$$X(W_0,\sigma) \to x_0 + \delta$$

$$Y(W_0,\sigma) \to y_0 + \xi.$$

As a result, point $P(x_0,y_0)$ on Γ_σ goes to point $P'(x_0+\delta, y_0+\xi)$. Let the distance

between P and P' be D. Then

$$D = \sqrt{\delta^2 + \xi^2} \leq \delta\sqrt{2}$$

assuming $|\delta|$ is the larger of $|\delta|$ and $|\xi|$. It follows that an infinitesimal change in parameter W also results in an infinitesimal change in the value of the vector-valued function Γ_σ. Therefore Γ_σ is a connected curve. □

Proof of lemma 4: Let M be the center of mass of $\Gamma = (x(w),y(w))$ with coordinates (x_M,y_M). Then

$$x_M = \frac{\int_0^1 x(w)\,dw}{\int_0^1 dw} = \int_0^1 x(w)\,dw$$

$$y_M = \frac{\int_0^1 y(w)\,dw}{\int_0^1 dw} = \int_0^1 y(w)\,dw.$$

Let $\Gamma_\sigma = (X(W,\sigma), Y(W,\sigma))$ be an arc length evolved version of Γ with $N = (X_N, Y_N)$ as its center of mass. Observe that

$$X_N = \int_0^1 X(W,\sigma)\,dW = \int_0^1 \int_{-\infty}^{\infty} g(v,\sigma)x(W-v)\,dv\,dW = \int_{-\infty}^{\infty} g(v,\sigma)\Big(\int_0^1 x(W-v)\,dW\Big)\,dv$$

W covers Γ_σ exactly once. Therefore

$$\int_0^1 x(W-v)\,dW = x_M.$$

So

$$X_N = x_M.$$

Similarly

$$Y_N = y_M.$$

It follows that M and N are the same point. □

Proof of lemma 5: Since G is simple and convex, every line L tangent to G contains that curve in the left (or right) half-plane it creates. Since Γ is inside G, Γ is also contained in the same half-plane. Now rotate L and Γ so that L becomes parallel to the y axis. L is now described by the equation $x = c$. Since L does not intersect Γ, it follows that $x(w_0) \geq c$ for every point w_0 on Γ. Let Γ_σ be an arc

length evolved version of Γ. Every point of Γ_σ is a weighted average of all the points of Γ. Therefore $X(W_0,\sigma) \geq c$ for every point W_0 on Γ_σ and Γ_σ is also contained in the same half-plane. This result holds for *every* line tangent to G therefore Γ_σ is contained inside the intersection of all the left (or right) half-planes created by the tangent lines of G. It follows that Γ_σ is also inside G. □

Proof of theorem 1: The proof will first be given for the regular curvature scale space of Γ, then the modifications needed to apply the same proof to the resampled and renormalized curvature scale space images will be explained. The proof of this theorem for the regular curvature scale space image only was first given in [Mokhtarian 1989].

Section **I** shows that the derivatives at a point on a curvature zero-crossing contour provide homogeneous equations in the moments of the Fourier transforms of the coordinate functions of the curve. Section **II** shows that the moments are related to the coefficients of expansion of the coordinate functions of the curve in functions related to the Hermite polynomials. Section **III** shows that the moments at one curvature zero-crossing point can be related to the moments at other curvature zero-crossing points. Section **IV** shows that the quadratic equations obtained in section **I** can be converted into a homogeneous linear system of equations which can be solved uniquely for the curvature function of the curve.

I. Constraints from the curvature zero-crossing contours

Let $\Gamma = (x(u), y(u))$ be the arc-length parametrization of the curve with Fourier transform $\tilde{\Gamma} = (\tilde{x}(\omega), \tilde{y}(\omega))$. The Fourier transform of the Gaussian filter $G(u,t) = \frac{1}{\sqrt{2t}} e^{-u^2/4t}$ is $\tilde{G}(\omega) = e^{-\omega^2 t}$.

Let $\Gamma_{t_0} = (x(u,t_0), y(u,t_0))$ be a curve obtained by convolving $x(u)$ and $y(u)$ with $G(u,t_0)$. Assume that Γ_{t_0} is in C_∞. Such a t_0 exists since Γ is in C_1. The curvature zero-crossings in a neighborhood of t_0 are given by solutions of $\alpha(u,t) = 0$ where

$$\alpha(u,t) = \dot{x}(u,t)\ddot{y}(u,t) - \dot{y}(u,t)\ddot{x}(u,t)$$

where . represents derivative with respect to u. Using the convolution theorem, the terms in $\alpha(u,t)$ can be expressed as following:

$$\dot{x}(u,t) = \int e^{-\omega^2 t} e^{i\omega u} (i\omega) \tilde{x}(\omega)\, d\omega$$

$$\ddot{y}(u,t) = \int e^{-\omega^2 t} e^{i\omega u} (-\omega^2) \tilde{y}(\omega)\, d\omega$$

$$\dot{y}(u,t) = \int e^{-\omega^2 t} e^{i\omega u} (i\omega) \tilde{y}(\omega)\, d\omega$$

$$\ddot{x}(u,t) = \int e^{-\omega^2 t} e^{i\omega u} (-\omega^2) \tilde{x}(\omega)\, d\omega.$$

The Implicit Function Theorem guarantees that the contours $u(t)$ are C_∞ in a neighborhood of t_0. Let ξ be a parameter of the curvature zero-crossing contour. Then

$$\frac{d}{d\xi} = \frac{du}{d\xi}\frac{\partial}{\partial u} + \frac{dt}{d\xi}\frac{\partial}{\partial t}.$$

On the curvature zero-crossing contour, $\alpha = 0$ and $\frac{d^k}{d\xi^k}\alpha = 0$ for all integers k. Furthermore, since the curvature zero-crossing contour is known, all the derivatives of u and t with respect to ξ are known as well.

We can now compute the derivatives of α with respect to ξ at (u_0, t_0). The first derivative is given by:

$$\begin{aligned}
\frac{d}{d\xi}\alpha(u_0,t_0) = \frac{du}{d\xi}\Big(& \int e^{-\omega^2 t} e^{i\omega u} (i\omega)^3 \tilde{y}(\omega)\, d\omega \int e^{-\omega^2 t} e^{i\omega u} (i\omega) \tilde{x}(\omega)\, d\omega \\
& - \int e^{-\omega^2 t} e^{i\omega u} (i\omega)^3 \tilde{x}(\omega)\, d\omega \int e^{-\omega^2 t} e^{i\omega u} (i\omega) \tilde{y}(\omega)\, d\omega \Big) \\
+ \frac{dt}{d\xi}\Big(& \int e^{-\omega^2 t} e^{i\omega u} (i\omega)^3 \tilde{x}(\omega)\, d\omega \int e^{-\omega^2 t} e^{i\omega u} (-\omega^2) \tilde{y}(\omega)\, d\omega \\
& + \int e^{-\omega^2 t} e^{i\omega u} (\omega^4) \tilde{y}(\omega)\, d\omega \int e^{-\omega^2 t} e^{i\omega u} (i\omega) \tilde{x}(\omega)\, d\omega \\
& - \int e^{-\omega^2 t} e^{i\omega u} (i\omega)^3 \tilde{y}(\omega)\, d\omega \int e^{-\omega^2 t} e^{i\omega u} (-\omega^2) \tilde{x}(\omega)\, d\omega \\
& - \int e^{-\omega^2 t} e^{i\omega u} \omega^4 \tilde{x}(\omega)\, d\omega \int e^{-\omega^2 t} e^{i\omega u} (i\omega) \tilde{y}(\omega)\, d\omega \Big).
\end{aligned} \tag{A.1}$$

Note that the moment of order k of function $f(\omega) = e^{-\omega^2 t} e^{i\omega u} (i\omega) \tilde{x}(\omega)$ is defined by:

$$M_k = \int_{-\infty}^{\infty} (i\omega)^k e^{-\omega^2 t} e^{i\omega u} (i\omega) \tilde{x}(\omega)\, d\omega$$

and the moment of order k of function $f'(\omega) = e^{-\omega^2 t} e^{i\omega u} (i\omega) \tilde{y}(\omega)$ is defined by:

$$M'_k = \int_{-\infty}^{\infty} (i\omega)^k e^{-\omega^2 t} e^{i\omega u} (i\omega) \tilde{y}(\omega) d\omega.$$

As a result, equation (A.1) can be re-written as:

$$\frac{d}{d\xi}\alpha(u_0, t_0) = \frac{du}{d\xi}(M'_2 M_0 - M_2 M'_0) \tag{A.2}$$

$$+ \frac{dt}{d\xi}(M_2 M'_1 + M'_3 M_0 - M'_2 M_1 - M_3 M'_0).$$

Furthermore, the second derivative is given by:

$$\frac{d^2}{d\xi^2}\alpha(u_0, t_0) = \frac{d^2 u}{d\xi^2}(M'_2 M_0 - M_2 M'_0) \tag{A.3}$$

$$+ \frac{d^2 t}{d\xi^2}(M_2 M'_1 + M'_3 M_0 - M'_2 M_1 - M_3 M'_0)$$

$$+ \left(\frac{du}{d\xi}\right)^2 (M'_3 M_0 + M_1 M'_2 - M_3 M'_0 - M'_1 M_2)$$

$$+ 2\frac{du}{d\xi}\frac{dt}{d\xi}(M'_4 M_0 - M_4 M'_0)$$

$$+ \left(\frac{dt}{d\xi}\right)^2 (M_4 M'_1 + 2M'_3 M_2 + M'_5 M_0 - M'_4 M_1 - 2M_3 M'_2 - M_5 M'_0).$$

Since the parametric derivatives along the curvature zero-crossing contours are zero, equations (A.2) and (A.3) are equal to zero. Note that equation (A.2) is a quadratic equation in the first four moments of functions $f(\omega)$ and $f'(\omega)$ and equation (A.3) is a quadratic equation in the first six moments of those functions. In general, the k+1st equation, $\frac{d^k}{d\xi^k}\alpha(u, t) = 0$ is a quadratic equation in the first $2k$+2 moments of each of the functions $f(\omega)$ and $f'(\omega)$ or a total of $4k$+4 moments. Our axes are chosen such that $u_0 = 0$. The next section shows that the moments of $f(\omega)$ and $f'(\omega)$ are the coefficients a_k and b_k in the expression of functions $\dot{x}(u)$ and $\dot{y}(u)$ in functions related to the Hermite polynomials. Therefore, having computed the first n derivatives of α at (u_0, t_0), we have n+1 homogeneous equations in the first $4n$+4 coefficients a_k and b_k. To determine the a_k and b_k, we need $3n$+3 additional and independent equations which can be provided by considering three neighboring curvature zero-crossing contours at (u_1, t_0), (u_2, t_0), and (u_3, t_0).

II. The moments and the coefficients of expansion of $\dot{x}(u)$ and $\dot{y}(u)$

This section shows that the moments and the moment-pairs in equations

$\frac{d^k}{d\xi^k}\alpha(u,t)$ are related respectively to the coefficients of the expression of the functions $\dot{x}(u)$, $\dot{y}(u)$ and the curvature function of Γ, $\kappa(u)$, in functions related to the Hermite polynomials. Expand function

$$\dot{x}(u) = \frac{d}{du}x(u)$$

in terms of the functions $\phi_k(u,\sigma)$ related to the Hermite polynomials $H_k(u)$ by

$$\phi_k(u,\sigma) = (-1)^k \frac{\sigma^{k-1}}{(\sqrt{2})^{k+1}\sqrt{\pi}} H_k(\frac{u}{\sigma\sqrt{2}})$$

$$H_k(u) = (-1)^k e^{u^2} \frac{d^k}{du^k} e^{-u^2}$$

$$\dot{x}(u) = \sum a_k(\sigma)\phi_k(u,\sigma).$$

The coefficients $a_k(\sigma)$ of the expansion are given by

$$a_k(\sigma) = <w_k(u,\sigma), \dot{x}(u)>$$

where $<,>$ denotes inner product in L^2 and $\{w_k(u,\sigma)\}$ is the set of functions biorthogonal to $\{\phi_k(u,\sigma)\}$. The $\{\phi_k(u,\sigma)\}$ are given explicitly by

$$\phi_k(u,\sigma) = \frac{\sigma^{2k-1}}{k!\sqrt{2\pi}} e^{\frac{u^2}{2\sigma^2}} \frac{d^k}{du^k} e^{-\frac{u^2}{2\sigma^2}}$$

and the $w_k(u,\sigma)$ by

$$w_k(u,\sigma) = (-1)^k \frac{d^k}{du^k} e^{-\frac{u^2}{2\sigma^2}}.$$

Since

$$\dot{x}(u) = \frac{1}{\sqrt{2\pi}} \int e^{i\omega u}(i\omega)\tilde{x}(\omega)\, d\omega$$

the a_k are given by

$$a_k(\sigma) = \frac{1}{\sqrt{2\pi}}(-1)^k \int < \frac{d^k}{du^k} e^{-\frac{u^2}{2\sigma^2}}, e^{i\omega u} > (i\omega)\tilde{x}(\omega)\, d\omega.$$

The inner product is just the inverse Fourier transform of $w_k(u,\sigma)$. Therefore

$$a_k(\sigma) = \int (i\omega)^k e^{\frac{-\omega^2\sigma^2}{2}} (i\omega)\,\tilde{x}(\omega)\, d\omega$$

which is equal to M_k modulus a factor $e^{i\omega u}$, since $t = \frac{\sigma^2}{2}$.

Similarly, the function

$$\dot{y}(u) = \frac{d}{du} y(u)$$

can be expanded in terms of the functions $\phi_k(u,\sigma)$ by

$$\dot{y}(u) = \sum b_k(\sigma)\,\phi_k(u,\sigma)$$

and it again follows that

$$b_k(\sigma) = \int (i\omega)^k e^{\frac{-\omega^2\sigma^2}{2}} (i\omega)\,\tilde{y}(\omega)\,d\omega$$

which is equal to M'_k modulus a factor $e^{i\omega u}$.

Furthermore, $a'_k(\sigma)$ and $b'_k(\sigma)$, the coefficients of expansion of functions $\ddot{x}(u)$ and $\ddot{y}(u)$ in terms of the functions $\phi_k(u,\sigma)$, can be seen to be related to $a_k(\sigma)$ and $b_k(\sigma)$ according to the following relationships:

$$a'_{k-1} = a_k(\sigma)$$

$$b'_{k-1} = b_k(\sigma).$$

Therefore $\kappa(u)$, the curvature function of Γ can be expressed as:

$$\begin{aligned}
\kappa(u) &= \dot{x}(u)\ddot{y}(u) - \dot{y}(u)\ddot{x}(u) \\
&= \sum a_k(\sigma)\phi_k(u,\sigma) \sum b'_k(\sigma)\phi_k(u,\sigma) - \sum b_k(\sigma)\phi_k(u,\sigma) \sum a'_k(\sigma)\phi_k(u,\sigma) \\
&= \sum\sum a_j(\sigma)b'_k(\sigma)\phi_j(u,\sigma)\phi_k(u,\sigma) - \sum\sum b_j(\sigma)a'_k(\sigma)\phi_j(u,\sigma)\phi_k(u,\sigma) \\
&= \sum\sum \left(a_j(\sigma)b_{k+1}(\sigma) - b_j(\sigma)a_{k+1}(\sigma)\right)\phi_j(u,\sigma)\phi_k(u,\sigma).
\end{aligned}$$

It follows that if the pairs $a_j(\sigma)b_k(\sigma)$, $j,k=0,\cdots,2n+1$, are all known, the curvature function of Γ can be reconstructed.

III. Combining information from more than one contours

To solve the system of equations obtained in section **I**, we need to obtain additional equations from other points of the curvature scale space image and relate them to the equations obtained from the first point. Suppose additional equations are obtained in the moments of functions $e^{-\omega^2 t}e^{i\omega u'}(i\omega)\tilde{x}(\omega)$ and $e^{-\omega^2 t}e^{i\omega u'}(i\omega)\tilde{y}(\omega)$ at point (u', t_0). We have

$$\dot{x}(u+u') = \int e^{i\omega u}e^{i\omega u'}(i\omega)\tilde{x}(\omega)\,d\omega = \sum c_k\phi_k(u)$$

and

$$\dot{y}(u+u') = \int e^{i\omega u} e^{i\omega u'} (i\omega) \tilde{y}(\omega) d\omega = \sum d_k \phi_k(u).$$

Now observe that

$$\sum c_k \phi_k(u) = \sum a_k \phi_k(u+u')$$

and

$$\sum d_k \phi_k(u) = \sum b_k \phi_k(u+u').$$

That is, $\phi_k(u+u')$ can be expressed as a linear combination of $\phi_j(u)$ with $j \leq k$ as has been shown in [Yuille and Poggio 1983].

IV. Reconstructing the curvature function

It was shown in section **I** that four points from four curvature scale space contours give us $4n+4$ equations in the first $2n+2$ moments of each of the functions $f(\omega)$ and $f'(\omega)$. The first $n+1$ equations form a system of homogeneous quadratic equations in the unknowns: $M_0(u), \cdots, M_{2n+1}(u)$ and $M'_0(u), \cdots, M'_{2n+1}(u)$. The other points, $u+u_k$, $1 \leq k \leq 3$, provide additional equations in the unknowns: $M_0(u+u_k), \cdots, M_{2n+1}(u+u_k)$ and $M'_0(u+u_k), \cdots, M'_{2n+1}(u+u_k)$. As shown in section **III**, the moments at $u+u_k$ can be expressed as a linear combination of the moments at u. Therefore it is possible to express all the equations in terms of the moments at u. The result is a system of $4n+4$ homogeneous quadratic equations in $4n+4$ unknowns. That system has at least one solution since the moments of order higher than $2n+1$ of $f(\omega)$ and $f'(\omega)$ are assumed to be zero. However, the solution obtained from a quadratic system of equations is in general not unique.

Equations (A.2) and (A.3) can be converted into homogeneous linear equations by assuming that each moment-pair appearing in those equations is a new variable. Table **2** shows the moment-pairs in equations (A.2) and (A.3). The + signs designate the moment-pairs in equation (A.2) and the + and x signs together designate the moment-pairs in equation (A.3).

	M'_0	M'_1	M'_2	M'_3	M'_4	M'_5
M_0			+	+	x	x
M_1			+		x	
M_2	+	+		x		
M_3	+		x			
M_4	x	x				
M_5	x					

Table **2**

Note that all other moment-pairs in table 2 can be computed from the existing ones using the following relationships:

$$M_iM'_j=\frac{M_{i-1}M'_j\cdot M_iM'_{j+1}}{M_{i-1}M'_{j+1}}=\frac{M_{i+1}M'_j\cdot M_iM'_{j+1}}{M_{i+1}M'_{j+1}}=\frac{M_iM'_{j-1}\cdot M_{i-1}M'_j}{M_{i-1}M'_{j-1}}=\frac{M_iM'_{j-1}\cdot M_{i+1}M'_j}{M_{i+1}M'_{j-1}}.$$

As before, we proceed to compute the first n derivatives at point (u_0, t_0) on one of the curvature zero-crossing contours. We now obtain $n+1$ homogeneous linear equations in some of the moment-pairs $M_iM'_j$ by assuming that each moment-pair is a new variable.

Since this system is in terms of the first $2n+2$ moments of functions $f(\omega)$ and $f'(\omega)$, it will contain $O(n^2)$ moment-pairs. Therefore additional equations are required to constrain the system. To obtain those equations, we proceed as follows:

Assume that moments of order higher than $2n+2$ are zero. Compute derivatives of order higher than n at (u_0, t_0) but set moments of order higher than $2n+2$ to zero in the resulting equations. If a sufficient number of derivatives are computed at (u_0, t_0), the number of equations obtained will be equal to the number of moment-pairs and our linear system will be constrained.

It follows from an assumption of generality that the system will have a unique zero eigenvector and therefore a unique solution modulus scaling. Once the moment-pairs in the system are known, all other moment-pairs can be computed from the known ones using the relationships given above. Since all the moment-pairs $M_iM'_j$ together determine the curvature function of the curve, it follows that the curve can be determined modulus a rigid motion and constant scaling.

Yuille and Poggio [1983] have shown that a 1-D signal can be reconstructed using two points from its scale space image. Note that our result implies that only one point is sufficient for the reconstruction of that signal.

The theorem has now been proven for the regular curvature scale space image. To prove the same result about the resampled curvature scale space, recall that derivatives at one point (at any scale) on any curvature zero-crossing contour in the curvature scale space of Γ were computed and it was shown that the resulting equations can be solved for the coefficients of expansion of the curvature function of Γ in functions related to the Hermite polynomials.

As before, we choose a point on a zero-crossing contour at any scale of the resampled curvature scale space image of Γ and compute the necessary derivatives. The value of σ in the resulting equations is then set to zero. Consequently,

the arc length evolved curve Γ_σ, where σ corresponds to the scale at which the derivatives were computed, is reconstructed modulus uniform scaling, rotation and translation.

The next step is to recover the original curve Γ. This is done by applying *reverse arc length evolution* to Γ_σ. Let the arc length evolved curve Γ_σ be defined by:

$$\Gamma_\sigma = \{(X(W,\sigma), Y(W,\sigma)) | W \in [0,1]\} .$$

A reverse arc length evolved curve Γ is defined by:

$$\Gamma = \{(x(w), y(w)) | w \in [0,1]\}$$

where

$$x(w) = X(w,\sigma) \circledast D_N(w,\sigma)$$

$$y(w) = Y(w,\sigma) \circledast D_N(w,\sigma)$$

where D_N is a deblurring operator defined in [Hummel *et al.* 1987] and

$$w(W,\sigma) = \int_0^\sigma \int_0^w \kappa^2(w,\sigma)\, dw d\sigma .$$

As a result, Γ is recovered modulo uniform scaling, rotation and translation.

To prove the same result about the renormalized curvature scale space image, evolved curve Γ_σ is again reconstructed. Then each of its coordinate functions is deblurred by convolving it with the deblurring operator D_N. Once again Γ is recovered modulo uniform scaling, rotation and translation. □

Proof of theorem 2: Since by assumption all evolved and arc length evolved curves Γ_σ are in C_2, the conditions of the implicit function theorem are satisfied on contours $\kappa(u,\sigma)$, $\kappa(w,\sigma)$ and $\kappa(W,\sigma) = 0$ in the resampled curvature scale space images of Γ. Since the proofs are identical, the theorem will be proven here for the regular curvature scale space image.

On any contour in the curvature scale space image

$$\kappa(u,\sigma) = 0.$$

Since all Γ_σ are in C_2 this is equivalent to:

$$\dot{X}(u,\sigma)\ddot{Y}(u,\sigma) - \ddot{X}(u,\sigma)\dot{Y}(u,\sigma) = 0.$$

To exploit the properties of the heat equation (Hummel *et al*, 1987), it is convenient to change variables and let

$$t = \frac{1}{2}\sigma^2.$$

So we define

$$x(u,t) = X(u,\sigma)$$

$$y(u,t) = Y(u,\sigma)$$

$$\alpha(u,t) = x_u(u,t)y_{uu}(u,t) - x_{uu}(u,t)y_u(u,t). \tag{A.4}$$

The functions $x(u,t)$ and $y(u,t)$ are obtained by convolving $\frac{1}{\sqrt{4\pi t}}e^{-(1/4t)u^2}$ with the original curve coordinates $x(u)$ and $y(u)$ respectively, and so they satisfy the heat equation:

$$x_{uu}(u,t) = x_t(u,t) \tag{A.5}$$

$$y_{uu}(u,t) = y_t(u,t). \tag{A.6}$$

On contours $\alpha\,(u,t) = 0$:

$$t = t(u)$$

$$\dot{t}(u) = \frac{dt}{du} = \frac{-\alpha_u}{\alpha_t}.$$

The theorem will be proven if we can show that for all points such that $\dot{t}(u) = 0$ we have $\ddot{t}\,(u) < 0$. Now,

$$\dot{t}(u) = 0 \tag{A.7}$$

if and only if

$$\alpha_u(u,t) = 0.$$

At an extremum where (A.7) holds, we have

$$\ddot{t}(u) = \frac{d}{du}\Big(\frac{-\alpha_u}{\alpha_t}\Big) = \frac{\partial}{\partial u}\Big(\frac{-\alpha_u}{\alpha_t}\Big) + \frac{\partial}{\partial t}\Big(\frac{-\alpha_u}{\alpha_t}\Big)\frac{dt}{du} = \frac{-\alpha_{uu}}{\alpha_t}.$$

So we must show that if

$$\alpha(u,t) = \alpha_u(u,t) = 0$$

then

$$\frac{\alpha_{uu}}{\alpha_t} > 0.$$

We shall show that these conditions require $\frac{\alpha_{uu}}{\alpha_t} = 1$ which proves the theorem.

From (A.4), (A.5) and (A.6) we have

$$\alpha = x_u y_t - x_t y_u$$

$$\alpha_u = x_{uu} y_t + x_u y_{ut} - x_{ut} y_u - x_t y_{uu}.$$

But using (A.5)

$$\alpha_u = x_u y_{ut} - x_{ut} y_u. \tag{A.8}$$

Similarly

$$\alpha_{uu} = (x_u y_{tt} - x_{tt} y_u) + (x_t y_{ut} - x_{ut} y_t).$$

If $\alpha = \alpha_u = 0$ then using (A.4) and (A.8)

$$x_t y_{ut} - x_{ut} y_t = x_t\Big(y_{ut} - x_{ut}\frac{y_t}{x_t}\Big) = x_t\Big(y_{ut} - x_{ut}\frac{y_u}{x_u}\Big) = \frac{x_t}{x_u}(x_u y_{ut} - x_{ut} y_u) = 0$$

so

$$\alpha_{uu} = x_u y_{tt} - x_{tt} y_u.$$

We also have

$$\alpha_t = (x_u y_{tt} - x_{tt} y_u) - (x_t y_{ut} - x_{ut} y_t)$$

so

$$\alpha_t = x_u y_{tt} - x_{tt} y_u$$

and hence $\alpha_{uu} = \alpha_t$ as claimed.

Notice, incidentally, that $\alpha(u,t)$ satisfies the diffusion equation at the maxima of the contours and that all such contours have a curvature of –1 at their maxima in (u,t) curvature scale space. □

Proof of theorem 3: It will be shown that this theorem holds for an arbitrary parametrization of Γ_σ. Therefore it must also be true of arc length parametrization or close approximations.

Let $(X(u,\sigma),\ Y(u,\sigma))$ be an arbitrary parametrization of Γ_σ. Since the class of polynomial functions is closed under convolution with a Gaussian [Hummel *et al.*, 1987], it follows that $X(u,\sigma)$ and $Y(u,\sigma)$ are also polynomial functions:

$$X(u,\sigma) = a_0 + a_1 u + a_2 u^2 + a_3 u^3 + \cdots$$

$$Y(u,\sigma) = b_0 + b_1 u + b_2 u^2 + b_3 u^3 + \cdots$$

Suppose that Γ_σ goes through the origin of the coordinate system at u=0. It follows that a_0=b_0=0. Assume further that there is a singularity on Γ_σ at u=0. We have:

$$X_u(u,\sigma) = a_1 + 2a_2u + 3a_3u^2 + 4a_4u^3 + \cdots$$

$$Y_u(u,\sigma) = b_1 + 2b_2u + 3b_3u^2 + 4b_4u^3 + \cdots$$

Since $X_u(u,\sigma)$ and $Y_u(u,\sigma)$ are zero at a singular point, it also follows that $a_1{=}b_1{=}0$.

We will now perform a case analysis of the singular point at $u = 0$ to determine when it corresponds to a cusp point. Since we will examine a small neighborhood of point $u = 0$, we will approximate the curve using the lowest degree terms in $X(u,\sigma)$ and $Y(u,\sigma)$:

$$\Gamma_\sigma = (u^m,\ u^n).$$

Assume w.l.o.g. that $n > m$. From above we know that $m > 1$.

Using

$$\mathbf{r}_u(u,\sigma) = (X_u(u,\sigma),\ Y_u(u,\sigma)) = (m\,u^{m-1},\ n\,u^{n-1})$$

it follows that

$$\mathbf{r}_u(\epsilon,\sigma) = (m\epsilon^{m-1},\ n\epsilon^{n-1}) = \epsilon^{m-1}(m,\ n\epsilon^{n-m})$$

and

$$\mathbf{r}_u(-\epsilon,\sigma) = (m(-\epsilon)^{m-1},\ n(-\epsilon)^{n-1}).$$

We can now analyze the singular point in each of the four possible cases:

1. m and n are both even numbers.

m–1 and n–1 are both odd numbers. Therefore

$$\mathbf{r}_u(-\epsilon,\sigma) = (-m\epsilon^{m-1},\ -n\epsilon^{n-1}) = -\epsilon^{m-1}(m,\ n\epsilon^{n-m}).$$

A comparison of $\mathbf{r}_u(\epsilon,\sigma)$ and $\mathbf{r}_u(-\epsilon,\sigma)$ shows that an infinitesimal change in the parameter u results in a large change in the direction of the tangent vector. Therefore the singular point *is* also a cusp point in this case.

2. m and n are both odd.

m–1 and n–1 are both even. Hence

$$\mathbf{r}_u(-\epsilon,\sigma) = (m\epsilon^{m-1},\ n\epsilon^{n-1}) = \epsilon^{m-1}(m,\ n\epsilon^{n-m}).$$

Comparing $\mathbf{r}_u(\epsilon,\sigma)$ to $\mathbf{r}_u(-\epsilon,\sigma)$ now shows that the tangent direction does not change with u in a small neighborhood of the singular point. Therefore this singular point is *not* a cusp point.

3. m is odd and n is even.

m–1 is even and n–1 is odd. Hence

$$\mathbf{r}_u(-\epsilon,\sigma) = (m\epsilon^{m-1},\ -n\epsilon^{n-1}) = \epsilon^{m-1}(m,\ -n\epsilon^{n-m}).$$

An infinitesimal change in u also results in an infinitesimal change in the tangent direction. Again, this singular point is *not* a cusp point.

4. m is even and n is odd.

m–1 is odd and n–1 is even. So

$$\mathbf{r}_u(-\epsilon,\sigma) = (-m\epsilon^{m-1},\ n\epsilon^{n-1}) = \epsilon^{m-1}(-m,\ n\epsilon^{n-m}).$$

An infinitesimal change in u now results in a large change in the tangent direction. Therefore this singular point *is* a cusp point.

It follows from the case analysis above that only the singular points in cases **1** and **4** are cusp points. We will now derive analytical expressions for the curve $\Gamma_{\sigma-\delta}$ so that it can be analyzed in a small neighborhood of the cusp point.

To deblur function $f(u) = u^k$, we convolve a rescaled version of that function with the function $\frac{2}{\sqrt{\pi}}e^{-x^2}(1-x^2)$, an approximation to the deblurring operator derived in (Hummel *et al.*, 1987) good for small amounts of deblurring , as follows:

$$(D_t f)(y) = \int_{-\infty}^{\infty} \frac{2}{\sqrt{\pi}} e^{-x^2}(1-x^2) f(y+2x\sqrt{t}\,)\,dx$$

or

$$(D_t f)(y) = \frac{2}{\sqrt{\pi}} \int_{-\infty}^{\infty} e^{-x^2}(1-x^2)(y+2x\sqrt{t}\,)^k dx$$

where t is the scale factor and controls the amount of deblurring. Solving the integral above yields

$$(D_t f)(y) = \sum_{\substack{p=0 \\ (p\ even)}}^{k} 1.3.5 \cdots (p-1) \frac{(2t)^{p/2}\ k(k-1) \cdots (k-p+1)}{p!} (1-p) y^{k-p}. \quad \text{(A.9)}$$

The following are four functions of the form $f(u) = u^k$ and their deblurred versions:

a. $f(u) = u^2$	$(D_t f)(u) = u^2 - 2t$
b. $f(u) = u^3$	$(D_t f)(u) = u^3 - 6tu$
c. $f(u) = u^4$	$(D_t f)(u) = u^4 - 12tu^2 - 36t^2$
d. $f(u) = u^5$	$(D_t f)(u) = u^5 - 20tu^3 - 180t^2u$.

We can now analyze the cusp points identified in cases 1 and 4 above. In case 1, the curve Γ_σ is approximated by (u^m, u^n) where m and n are both even numbers. We now deblur the curve to obtain:

$$(D_t x)(u) = u^m - c_1 t u^{m-2} - c_2 t^2 u^{m-4} - \cdots - c_{\frac{m-2}{2}} t^{\frac{m-2}{2}} u^2 - c_{\frac{m}{2}} t^{\frac{m}{2}}$$

$$(D_t y)(u) = u^n - c'_1 t u^{n-2} - c'_2 t^2 u^{n-4} - \cdots - c'_{\frac{n-2}{2}} t^{\frac{n-2}{2}} u^2 - c'_{\frac{n}{2}} t^{\frac{n}{2}}.$$

Note that all powers of u are even and the constants c_j and c'_j are all positive as follows from an examination of (A.9). It follows that

$$(D_t \dot{x})(u) = m u^{m-1} - (m-2) c_1 t u^{m-3} - \cdots - 2 c_{\frac{m-2}{2}} t^{\frac{m-2}{2}} u$$

$$(D_t \dot{y})(u) = n u^{n-1} - (n-2) c'_1 t u^{n-3} - \cdots - 2 c'_{\frac{n-2}{2}} t^{\frac{n-2}{2}} u$$

contain only odd powers of u and $(D_t \dot{\mathbf{r}})(\epsilon) = -(D_t \dot{\mathbf{r}})(-\epsilon)$. Hence there is also a cusp point on the curve $\Gamma_{\sigma-\delta}$ at $u_0 = 0$. In fact, the cusp point must also exist on Γ itself. This is a contradiction of the assumption that Γ is in C_2. It follows that Γ_σ can not have a cusp point of this kind at u_0.

We shall now turn to the cusp points encountered in case 4. Recall that, in that case, the curve Γ_σ is approximated, in a small neighborhood of the cusp point, by (u^m, u^n) where m is even and n is odd. Again we deblur the curve to obtain:

$$(D_t x)(u) = u^m - c_1 t u^{m-2} - c_2 t^2 u^{m-4} - \cdots - c_{\frac{m-2}{2}} t^{\frac{m-2}{2}} u^2 - c_{\frac{m}{2}} t^{\frac{m}{2}}$$

$$(D_t y)(u) = u^n - c'_1 t u^{n-2} - c'_2 t^2 u^{n-4} - \cdots - c'_{\frac{n-1}{2}} t^{\frac{n-1}{2}} u.$$

Again note that constants c_j and c'_j are all positive.

The deblurred curve intersects itself if there are two values of u, u_1 and u_2, such that

$$x(u_1) = x(u_2) \tag{A.10}$$

$$y(u_1) = y(u_2). \tag{A.11}$$

Since $(D_t x)(u)$ contains even powers of u only, it follows from (A.10) that

$u_1 = -u_2$. Since $(D_t y)(u)$ contains odd powers of u only, substituting $u_1 = -u_2$ in (A.11) and simplifying yields:

$$u_1{}^n - c'_1 t u_1{}^{n-2} - c'_2 t^2 u_1{}^{n-4} - \cdots - c'_{\frac{n-1}{2}} t^{\frac{n-1}{2}} u_1 = 0.$$

Since $\Gamma_{\sigma-\delta}$ is of interest to us, we let $t = \delta$. We now obtain

$$u_1{}^n - c'_1 \delta u_1{}^{n-2} - c'_2 \delta^2 u_1{}^{n-4} - \cdots - c'_{\frac{n-1}{2}} \delta^{\frac{n-1}{2}} u_1 = 0. \qquad \text{(A.12)}$$

$u_1 = 0$ is one of the roots of this equation. For very small values of u_1, the LHS of (A.12) is negative since the first term will be smaller than each of the other terms (which are negative). As u_1 grows larger, the first term becomes larger than the sum of all other terms and therefore the LHS of (A.12) becomes positive. It follows that there exists a positive value of u_1 at which (A.12) is satisfied. Therefore $\Gamma_{\sigma-\delta}$ is self-intersecting in a small neighborhood of the cusp point of Γ_σ. □

Proof of theorem 4: Assume by contradiction that Γ is a simple curve which intersects itself during arc length evolution. Γ must touch itself at point P before self-intersection. There are two distinct, non-overlapping neighborhoods of Γ which contain point P. Let these neighborhoods be S_1 and S_2. The coordinate functions of S_1 and S_2 can be represented polynomially. Assume that S_1 and S_2 have horizontal tangents at P and that S_1 is contained inside S_2. Let P be at the origin. It follows that S_1 and S_2 can be approximated using the lowest non-zero terms in the polynomial representation of their coordinate functions:

$$S_1 = (u^m, u^n)$$

$$S_2 = (u^p, u^q).$$

It follows that m, n, p and q are at least equal to one. It can be seen that $n>m$ and $q>p$. We will now find approximations to arc length parametrization of S_1 and S_2. On segment S_1:

$$X(u,\sigma) = u^m$$

$$Y(u,\sigma) = u^n.$$

Therefore

$$X_u(u,\sigma) = mu^{m-1}$$

$$Y_u(u,\sigma) = nu^{n-1}$$

and

$$s = \int_0^u \sqrt{X_u^2 + Y_u^2}\, du = \int_0^u \sqrt{m^2u^{2(m-1)} + n^2u^{2(n-1)}}\, du = \int_0^u mu^{m-1}(1 + \frac{n^2}{m^2}u^{2(n-m)})^{1/2}\, du.$$

It follows from Taylor's theorem that about u=0:

$$(1 + \frac{n^2}{m^2}u^{2(n-m)})^{1/2} \simeq 1 + \frac{n^2}{2m^2}u^{2(n-m)}\ .$$

Hence

$$s = \int_0^u (mu^{m-1} + \frac{n^2}{2m}u^{2n-m-1})du = u^m + \frac{n^2}{4nm-2m^2}u^{2n-m}.$$

It follows from the fact $n>m$ that $2n-m>m$. Therefore s can be approximated as:

$$s \simeq u^m$$

so

$$u \simeq (s)^{1/m}$$

and

$$u^n \simeq (s)^{n/m}$$

and an approximation to the arc length parametrization of S_1 at P is given by:

$$X(s,\sigma) = s$$

$$Y(s,\sigma) = (s)^{n/m}.$$

Now let $r = s-1$. Then

$$X(r,\sigma) = r+1$$

$$Y(r,\sigma) = (r+1)^{n/m}.$$

It follows from Taylor's theorem that about r=0:

$$Y(r,\sigma) \simeq 1 + \frac{n}{m}r + \frac{n}{2m}(\frac{n}{m}-1)r^2\ .$$

Therefore the new arc length parametrization of S_1 is given by:

$$X(r,\sigma) = 1 + r$$

$$Y(r,\sigma) = 1 + \frac{n}{m}r + \frac{n}{2m}(\frac{n}{m}-1)r^2.$$

We now deblur this arc length parametrization of S_1 by an infinitesimal amount t. On the deblurred segment:

$$X_1(r,\sigma) = 1 + r$$

$$Y_1(r,\sigma) = 1 + \frac{n}{m}r + \frac{n}{2m}(\frac{n}{m}-1)(r^2 - 2t).$$

Similarly, an arc length parametrization for the deblurred segment S_2 is given by:

$$X_2(r,\sigma) = 1 + r$$

$$Y_2(r,\sigma) = 1 + \frac{q}{p}r + \frac{q}{2p}(\frac{q}{p}-1)(r^2 - 2t).$$

Since S_1 is inside S_2, it follows that $\frac{n}{m}$ is larger than $\frac{q}{p}$. It follows that at r=0, Y_1 is less than Y_2. However, as r grows, Y_1 becomes larger than Y_2. Therefore the curve intersects itself just before touching itself. This is a contradiction of the assumption that the curve was simple before touching itself. It follows that a simple curve remains simple during arc length evolution. □

Proof of theorem 5: It will be shown that this theorem holds for an arbitrary parametrization of Γ_σ. Therefore it must also be true of arc length parametrization or close approximations.

Let $(x(u), y(u))$ be an arbitrary parametrization of Γ_σ with a cusp point at u_0. Using a case analysis similar to the one in the proof of theorem **3** to characterize all possible kinds of singularities of Γ_σ at u_0, we can again conclude that only the singular points in cases **1** and **4** are cusp points. In case **1**, the curve is approximated by (u^m, u^n) in a neighborhood of u_0 where m and n are both even. This type of cusp point can not arise on Γ_σ if Γ is in C_1. We now turn to the cusp points of case **4**. Recall that in case **4**, the curve Γ_σ is approximated, in a neighborhood of u_0, by (u^m, u^n) where m is even and n is odd. Observe that

$$\dot{x}(u) = m\,u^{m-1}$$

$$\ddot{x}(u) = m(m-1)\,u^{m-2}$$

$$\dot{y}(u) = n\,u^{n-1}$$

$$\ddot{y}(u) = n(n-1)\,u^{n-2}$$

and

$$\kappa(u) = \frac{\dot{x}(u)\ddot{y}(u) - \dot{y}(u)\ddot{x}(u)}{(\dot{x}(u)^2 + \dot{y}(u)^2)^{3/2}} = \frac{mn(n-1)\,u^{m+n-3} - m(m-1)n\,u^{m+n-3}}{(m^2u^{2m-2} + n^2u^{2n-2})^{3/2}}.$$

Since $n>m$, $\kappa(u)$ is always positive on either side of the cusp point in a neighborhood of u_0. Therefore no curvature zero-crossings exist in that neighborhood on Γ_σ.

We now derive analytical expressions for $\Gamma_{\sigma+\delta}$ so that it can be analyzed in a neighborhood of u_0. To blur function $f(u) = u^k$, we convolve a rescaled version of that function with the function $\frac{1}{\sqrt{\pi}}e^{-x^2}$, the deblurring operator, as follows:

$$F(u) = \int_{-\infty}^{\infty} \frac{1}{\sqrt{\pi}} e^{-x^2} f(u+2x\sqrt{t}\,)\,dx$$

or

$$F(u) = \frac{1}{\sqrt{\pi}} \int_{-\infty}^{\infty} e^{-x^2} (u+2x\sqrt{t}\,)^k dx$$

where t is the scale factor and controls the amount of blurring. Solving the integral above yields

$$F(u) = \sum_{\substack{p=0 \\ (p\ even)}}^{k} 1.3.5 \cdots (p-1) \frac{(2t)^{p/2} k(k-1) \cdots (k-p+1)}{p!} u^{k-p}.$$

The following are four functions of the form $f(u) = u^k$ and their blurred versions:

a. $f(u) = u^2$	$F(u) = u^2 + 2t$
b. $f(u) = u^3$	$F(u) = u^3 + 6tu$
c. $f(u) = u^4$	$F(u) = u^4 + 12tu^2 + 12t^2$
d. $f(u) = u^5$	$F(u) = u^5 + 20tu^3 + 60t^2u$.

An expression for $\Gamma_{\sigma+\delta}$ in a neighborhood of the cusp point can be obtained by by blurring each of its coordinate functions:

$$X(u) = u^m + c_1 t u^{m-2} + c_2 t^2 u^{m-4} + \cdots + c_{\frac{m-2}{2}} t^{\frac{m-2}{2}} u^2 + c_{\frac{m}{2}} t^{\frac{m}{2}}$$

$$Y(u) = u^n + c'_1 t u^{n-2} + c'_2 t^2 u^{n-4} + \cdots + c'_{\frac{n-1}{2}} t^{\frac{n-1}{2}} u.$$

Note that all constants are positive, all powers of u in $X(u)$ are even and all powers of u in $Y(u)$ are odd. It follows that all powers of u in

$$\dot{X}(u) = mu^{m-1} + (m-2)c_1 t u^{m-3} + \cdots + 2c_{\frac{m-2}{2}} t^{\frac{m-2}{2}} u$$

are odd, all powers of u in

$$\ddot{X}(u) = m(m-1)u^{m-2} + (m-2)(m-3)c_1 t u^{m-4} + \cdots + 2c_{\frac{m-2}{2}} t^{\frac{m-2}{2}}$$

are even, all powers of u in

$$\dot{Y}(u) = nu^{n-1} + (n-2)c'_1 tu^{n-3} + \cdots + c'_{\frac{n-1}{2}} t^{\frac{n-1}{2}}$$

are even and all powers of u in

$$\ddot{Y}(u) = n(n-1)u^{n-2} + (n-2)(n-3)c'_1 tu^{n-4} + \cdots + c'_{\frac{n-3}{2}} t^{\frac{n-3}{2}}$$

are odd.

The curvature of $\Gamma_{\sigma+\delta}$ in a neighborhood of u_0 is given by

$$\kappa(u) = \frac{\dot{X}(u)\ddot{Y}(u) - \dot{Y}(u)\ddot{X}(u)}{(\dot{X}(u)^2 + \dot{Y}(u)^2)^{3/2}}.$$

Since the denominator of $\kappa(u)$ never goes to zero in a neighborhood of u_0, the zero-crossings of $\kappa(u)$ are the same as those of

$$\kappa'(u) = \dot{X}(u)\ddot{Y}(u) - \dot{Y}(u)\ddot{X}(u).$$

Observe that the term with the highest power of u in $\dot{X}(u)\ddot{Y}(u)$ is $mn(n-1)u^{m+n-3}$ and the term with the highest power of u in $\dot{Y}(u)\ddot{X}(u)$ is $m(m-1)nu^{m+n-3}$ and that in both $\dot{X}(u)\ddot{Y}(u)$ and $\dot{Y}(u)\ddot{X}(u)$, all powers of u are even and all constants are positive. Furthermore, note that at $u=0$, $\dot{X}(u)\ddot{Y}(u)$ is zero and $\dot{Y}(u)\ddot{X}(u) > 0$. Therefore at $u=0$, $\kappa < 0$. As u grows larger in absolute value, the terms in $\dot{X}(u)\ddot{Y}(u)$ and $\dot{Y}(u)\ddot{X}(u)$ with highest powers of u become dominant (all other terms have positive powers of $t=\delta$ in them). Since the dominant terms have equal powers of u, the one with the larger coefficient becomes the larger term. Since $n > m$, the largest term in $\dot{X}(u)\ddot{Y}(u)$ becomes larger than the largest term in $\dot{Y}(u)\ddot{X}(u)$. Therefore as u grows in absolute value, κ becomes positive. It follows that there are two curvature zero-crossings in the neighborhood of u_0 on $\Gamma_{\sigma+\delta}$. These zero-crossings are new since it was shown that no zero-crossings exist in the neighborhood of u_0 on Γ_σ. □

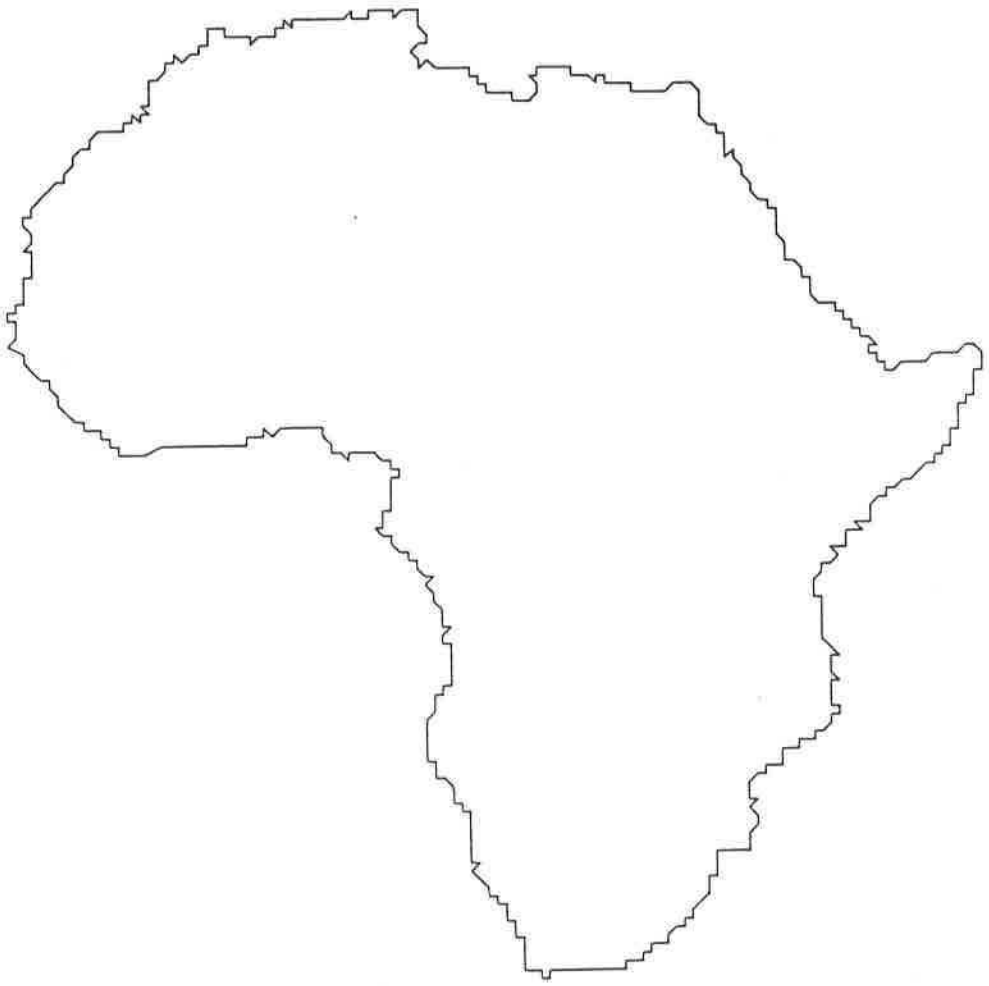

Figure 2.1. Coastline of Africa

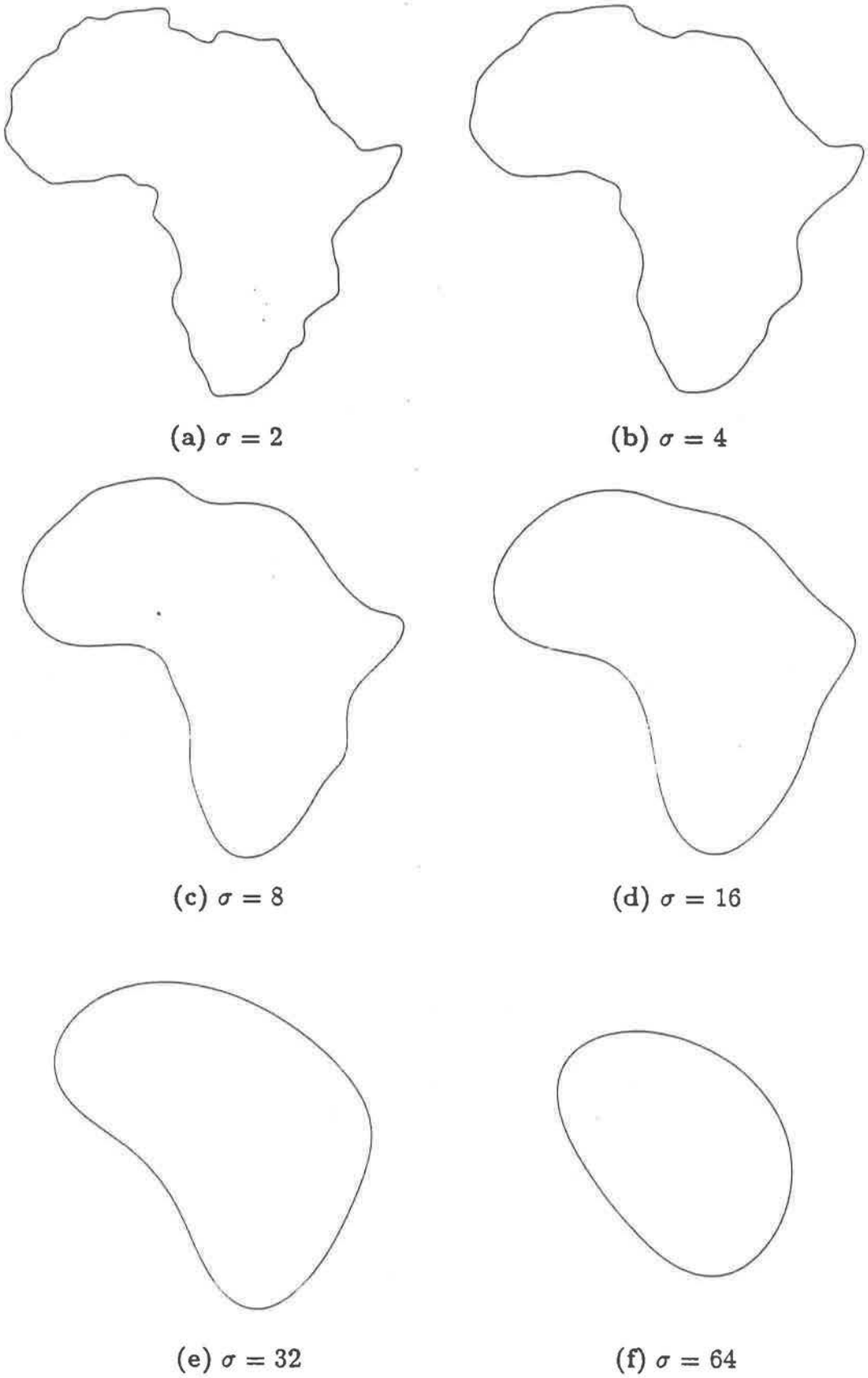

(a) $\sigma = 2$ (b) $\sigma = 4$

(c) $\sigma = 8$ (d) $\sigma = 16$

(e) $\sigma = 32$ (f) $\sigma = 64$

Figure 2.2. Africa during evolution

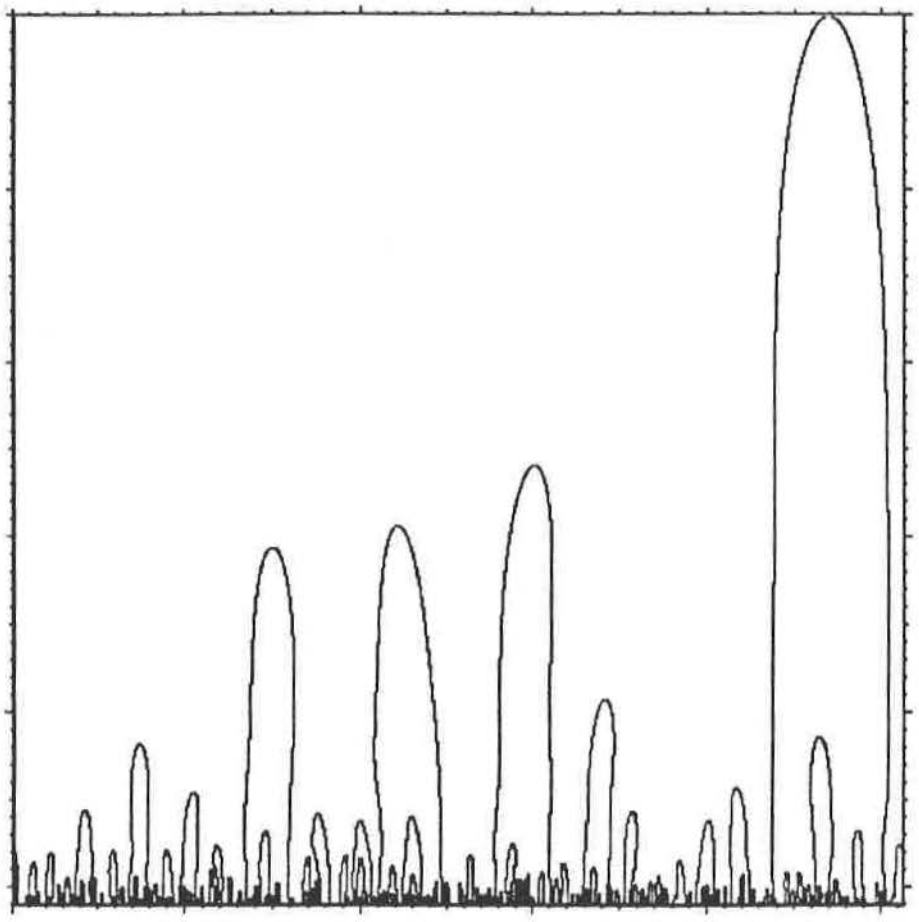

Figure 2.3. The Curvature Scale Space Image of Africa

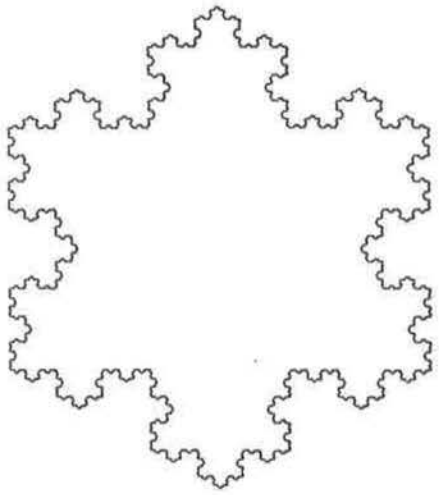

(a) The original curve

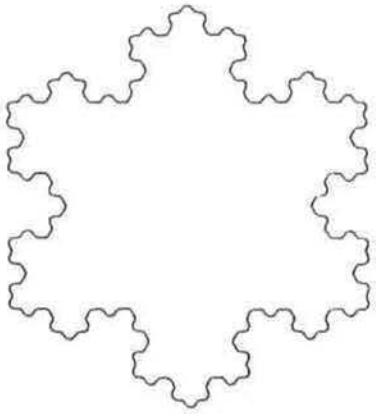

(b) $\sigma = 1$

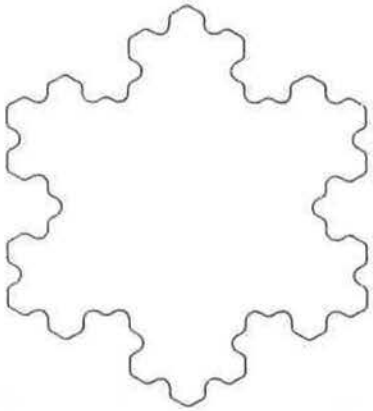

(c) $\sigma = 2$

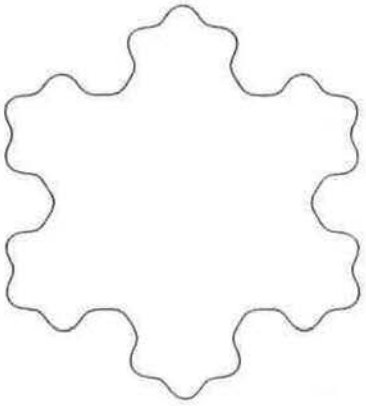

(d) $\sigma = 5$

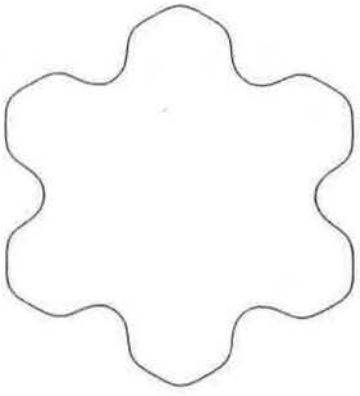

(e) $\sigma = 10$

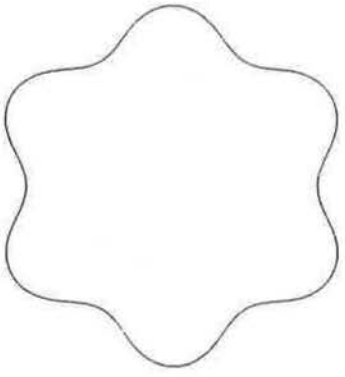

(f) $\sigma = 20$

Figure 2.4. Koch's snowflake curve during evolution

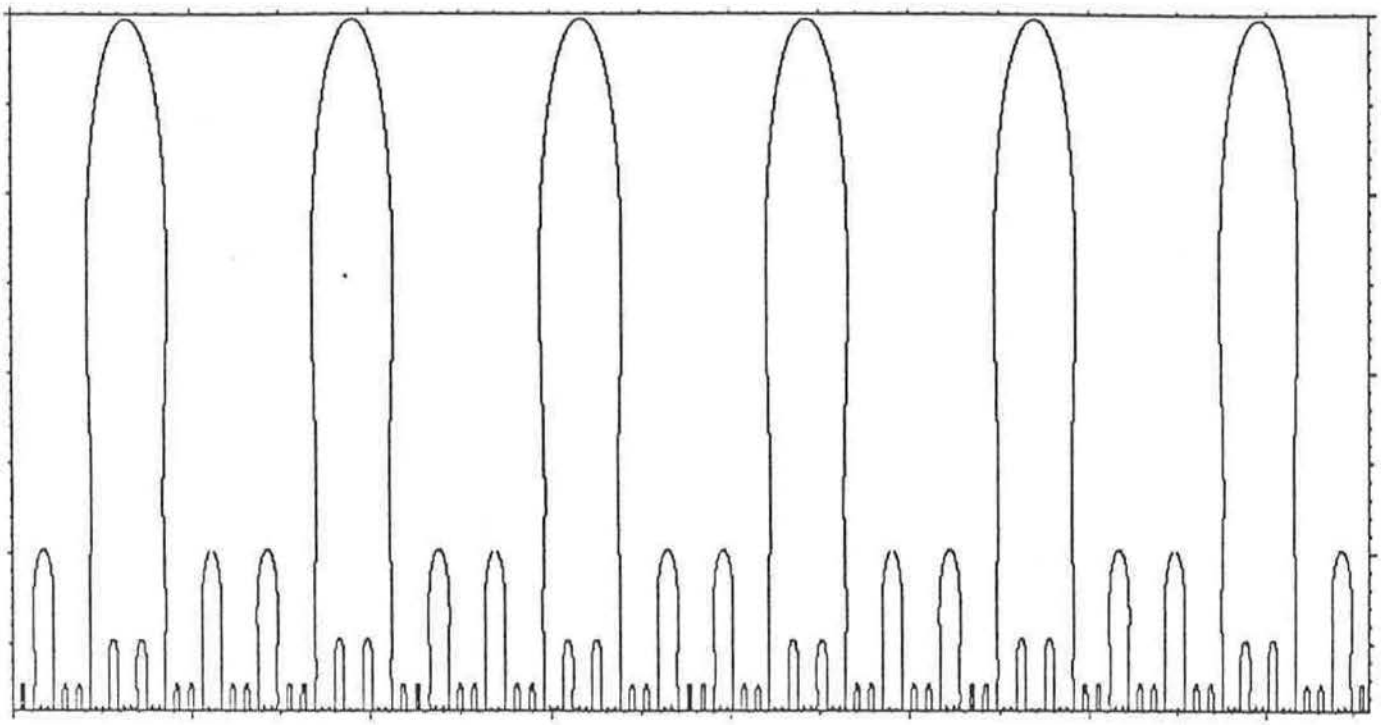

Figure 2.5. The Curvature Scale Space Image of the snowflake curve

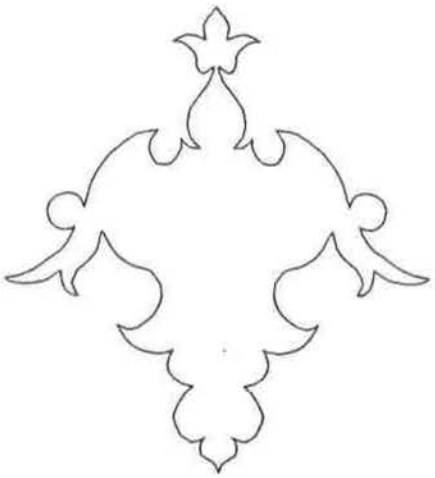

(a) The original curve

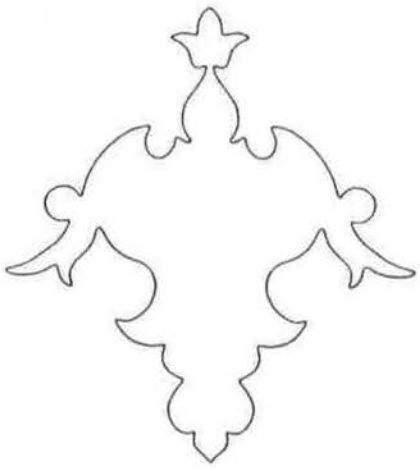

(b) $\sigma = 2$

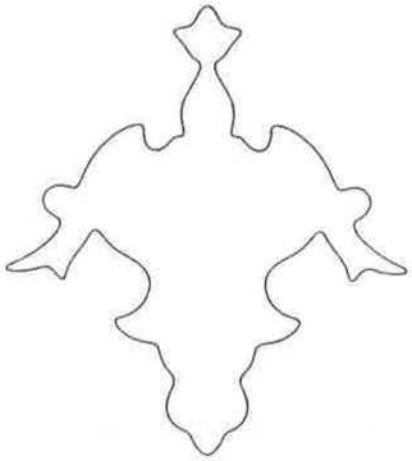

(c) $\sigma = 5$

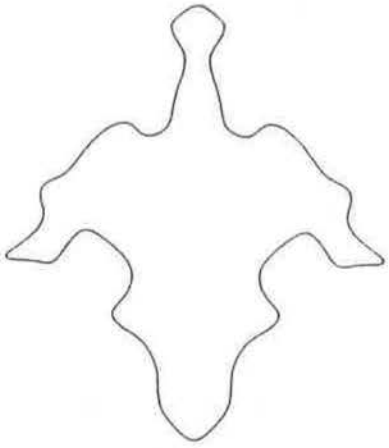

(d) $\sigma = 10$

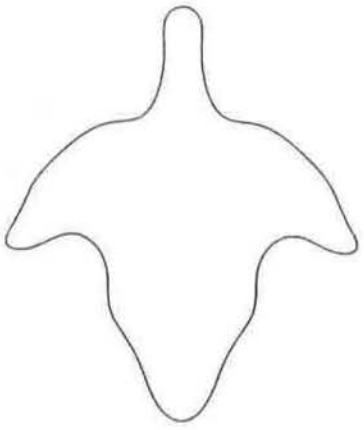

(e) $\sigma = 20$

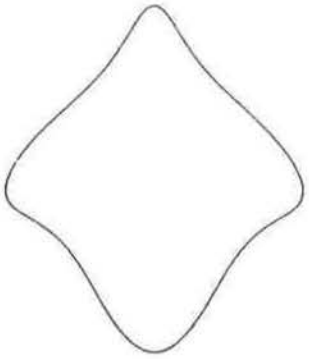

(f) $\sigma = 50$

Figure 2.6. A design from a Persian carpet during evolution

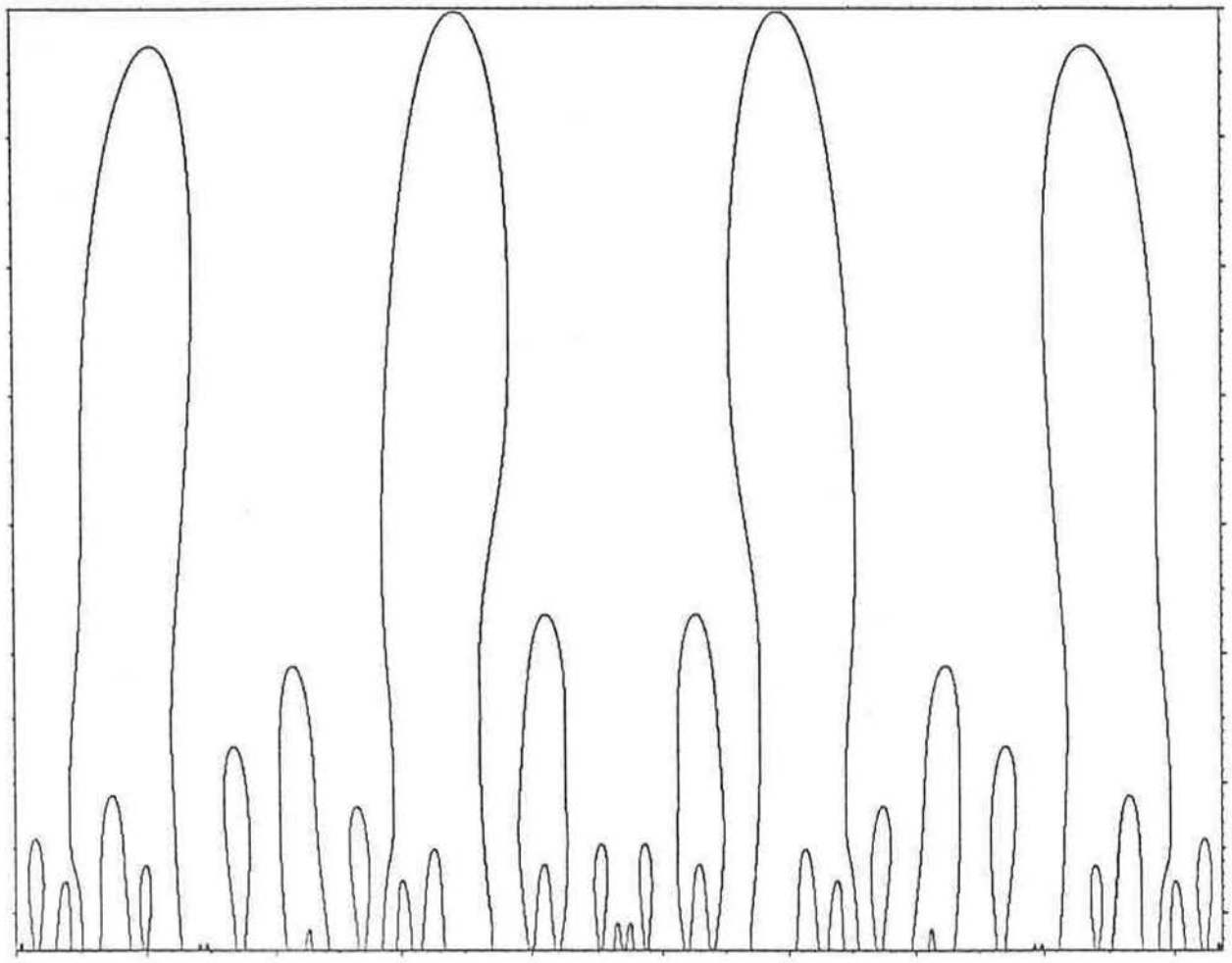

Figure 2.7. The curvature scale space image of the carpet design.

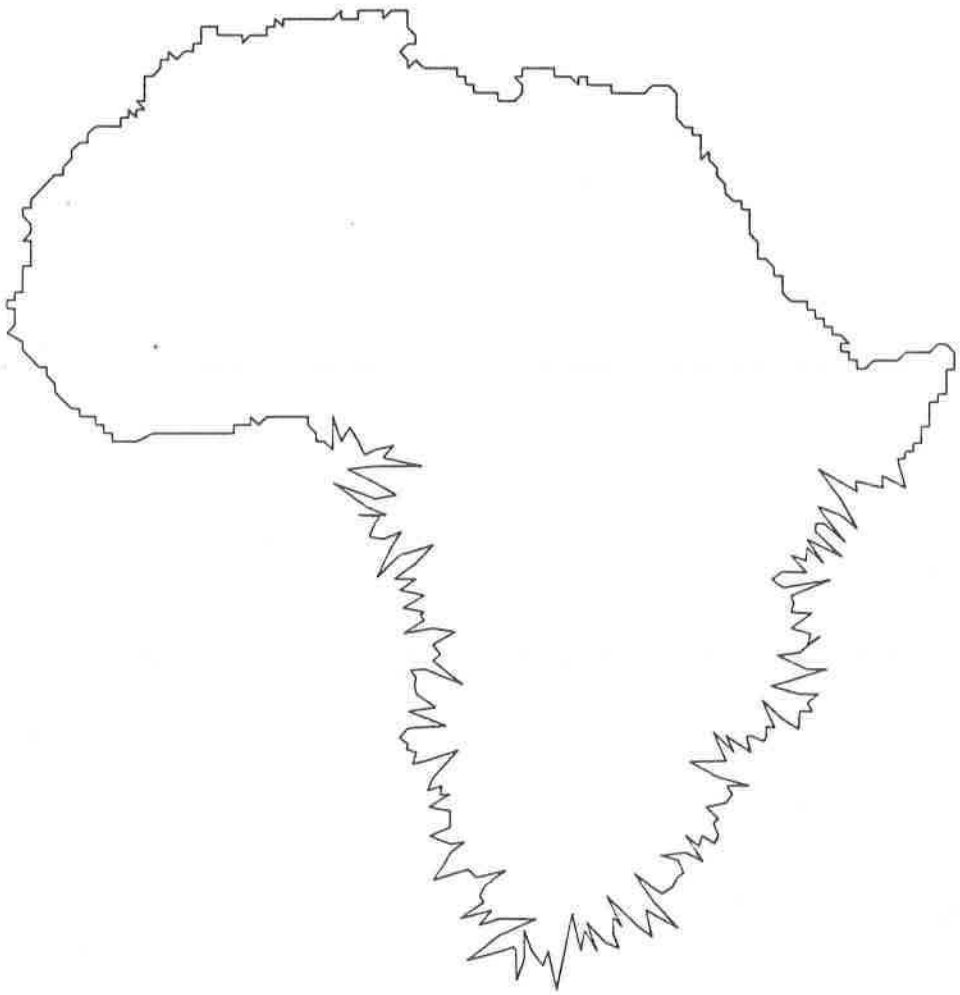

Figure 3.1. Coastline of Africa with noise

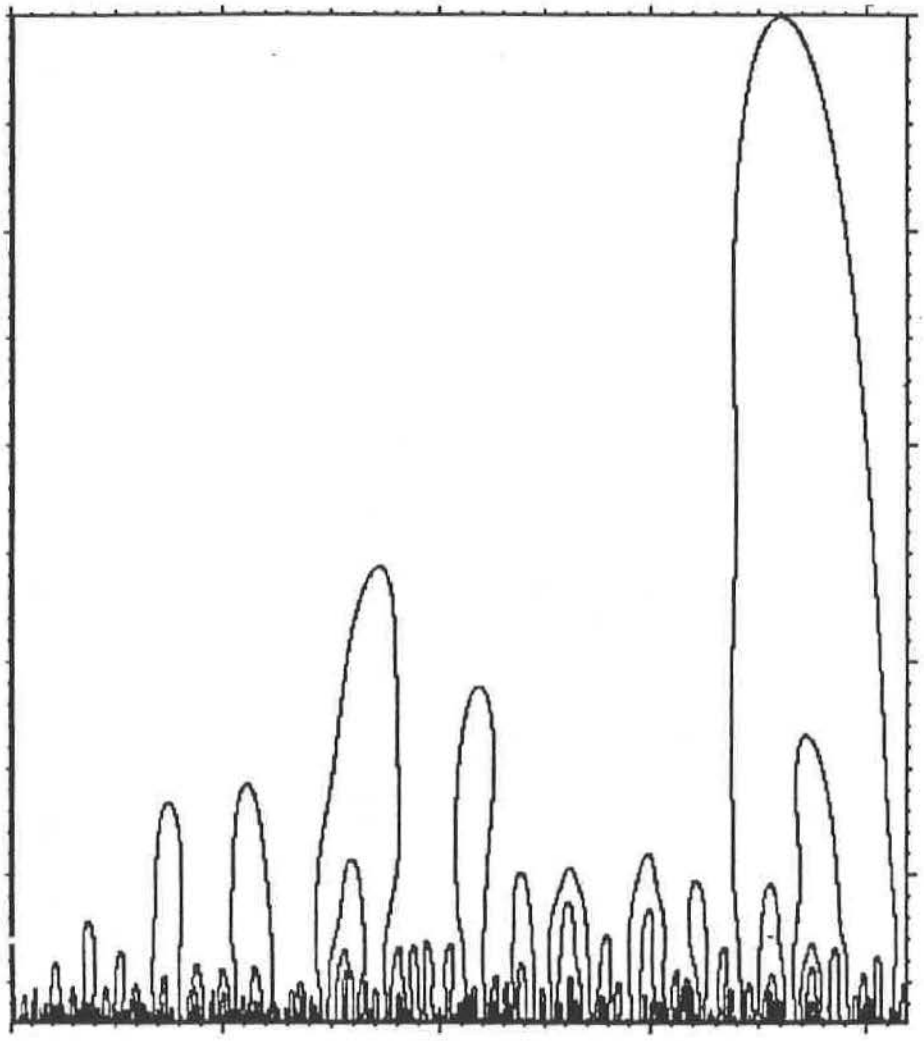

Figure 3.2. The Curvature Scale Space Image of Africa with noise

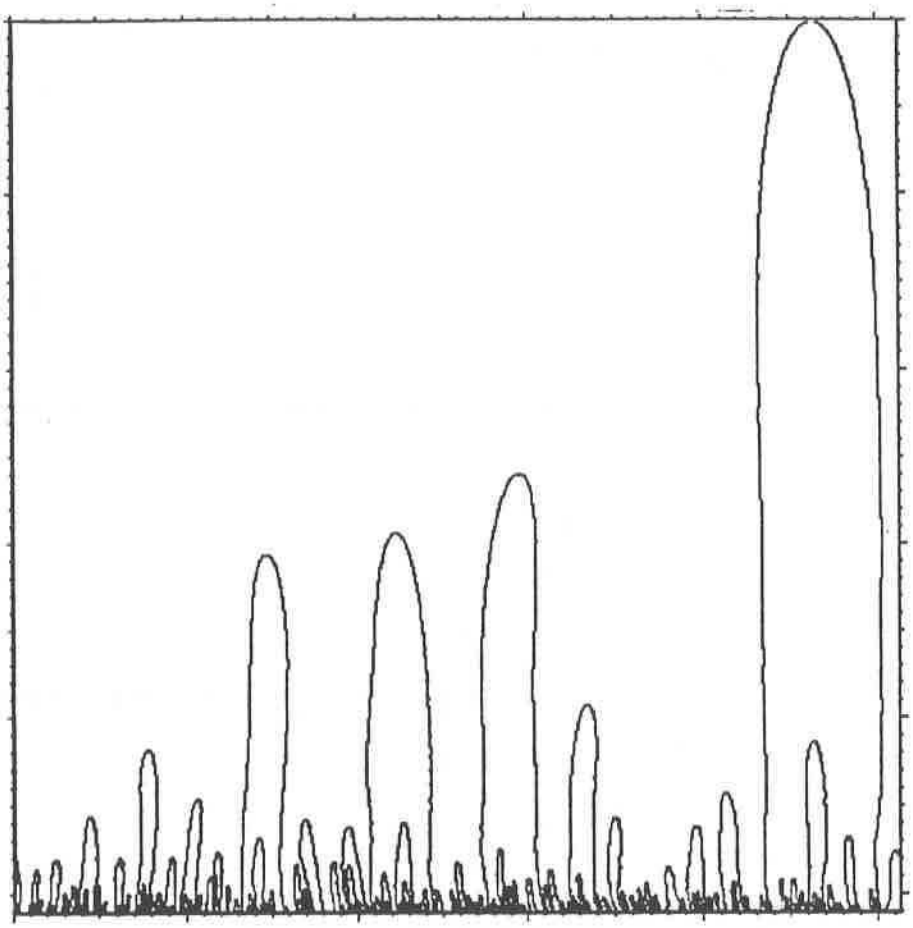

Figure 3.3. The Renormalized Curvature Scale Space Image of Africa

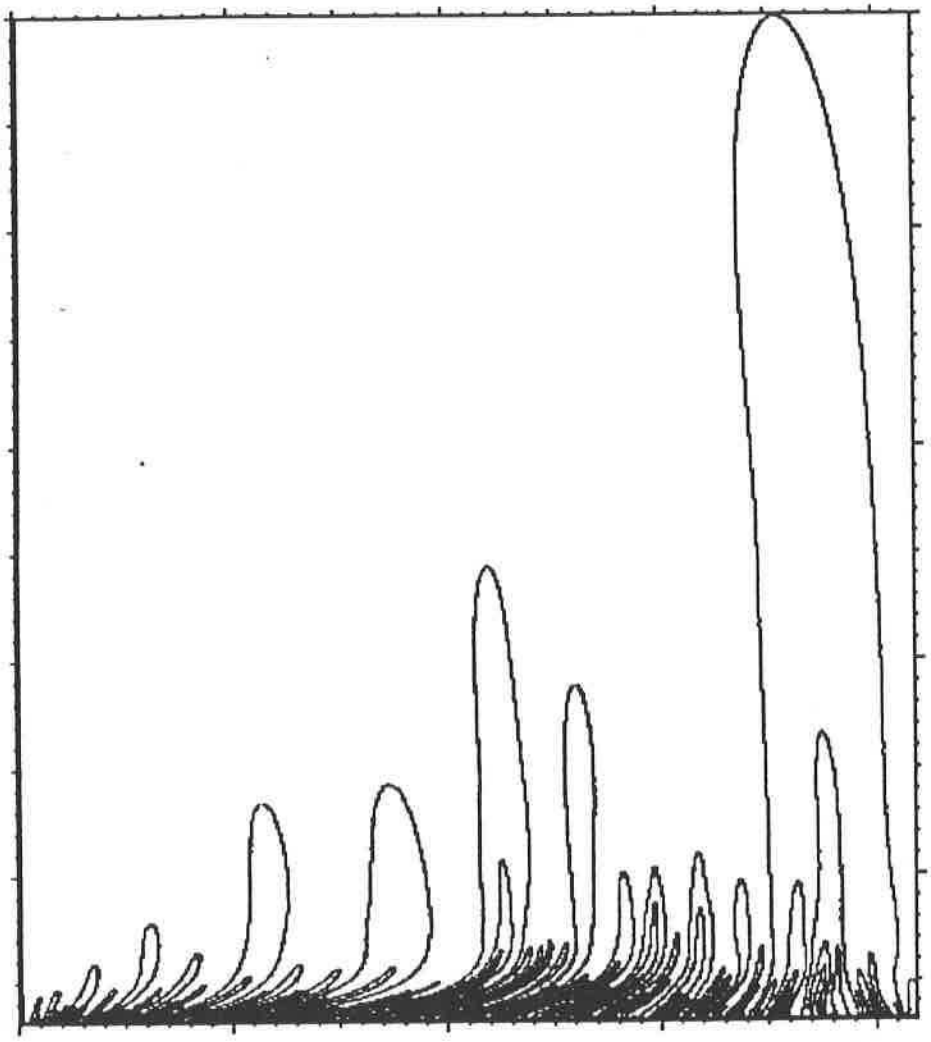

Figure 3.4. The Renormalized Curvature Scale Space Image of noisy Africa

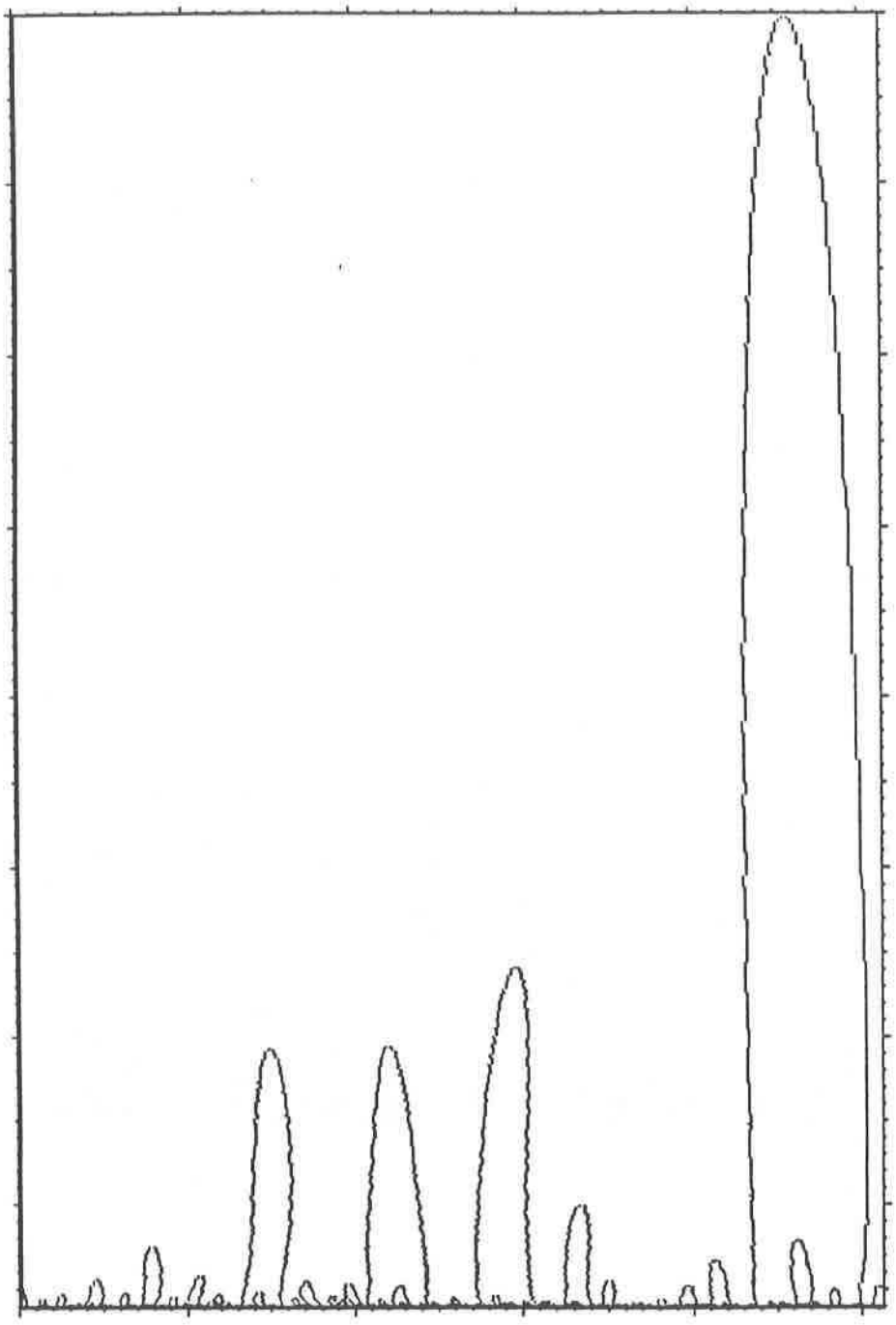

Figure 4.1. The Resampled Curvature Scale Space Image of Africa

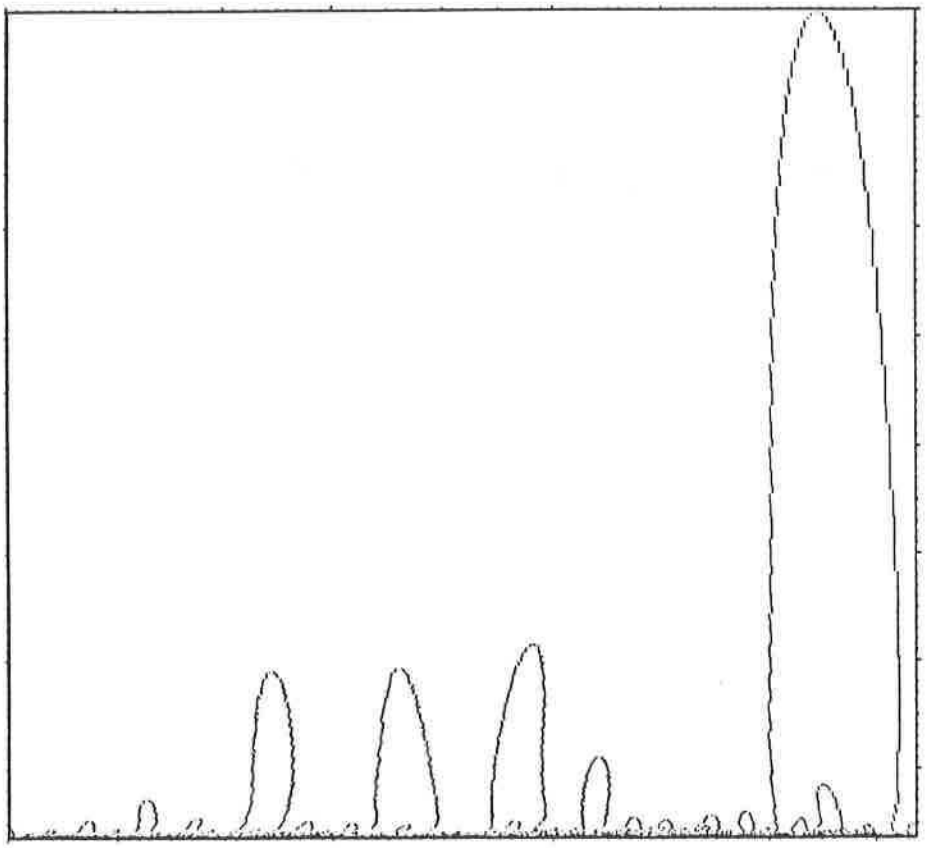

Figure 4.2. The Resampled Curvature Scale Space Image of noisy Africa

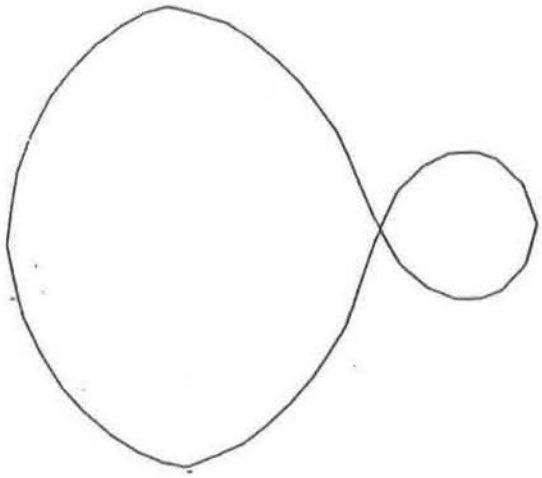

(a) A self-crossing curve

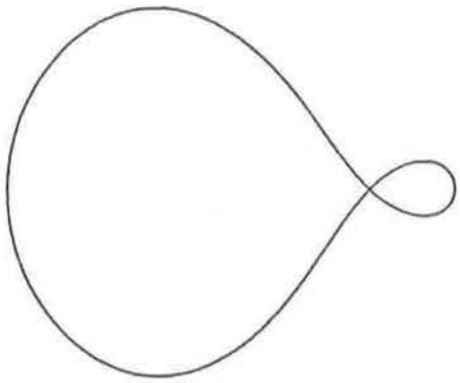

(b) Convolved with σ=8

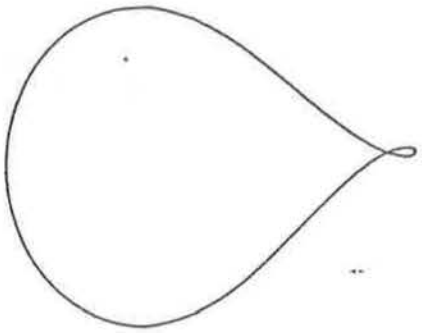

(c) Convolved with σ=12

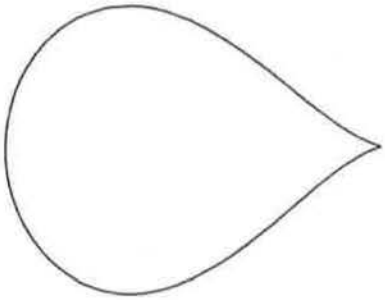

(d) Convolved with σ=14

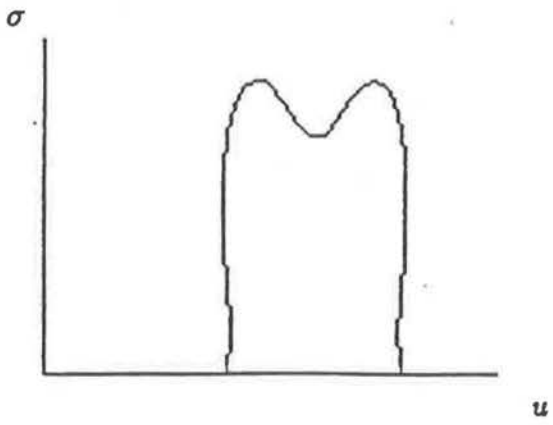

(e) The curvature scale-space image of the curve

Figure 6.1. A self-crossing curve during evolution

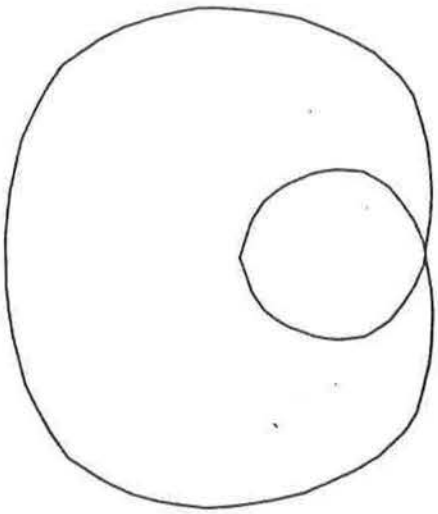

(a) A convex curve

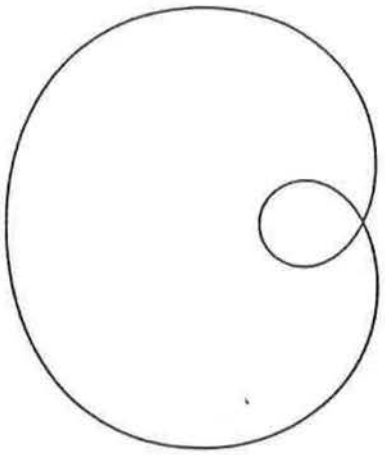

(b) Convolved with σ=16

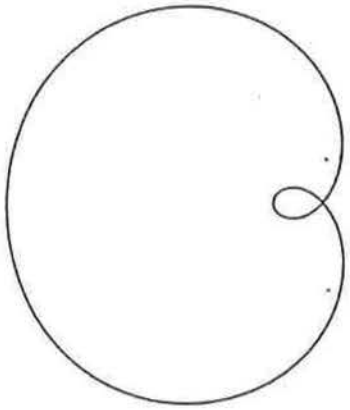

(c) Convolved with σ=24

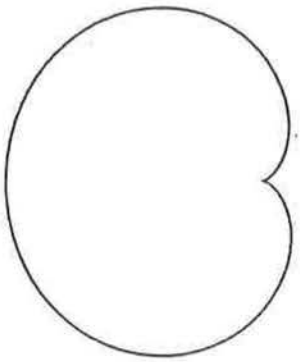

(d) Convolved with σ=32

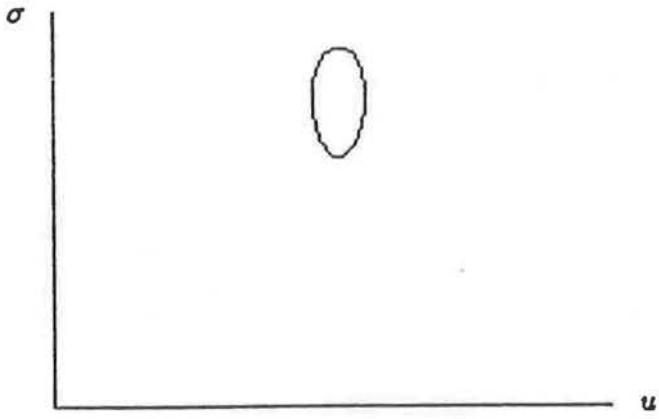

(e) The curvature scale-space image of the curve

Figure 6.2. A convex but self-crossing curve during evolution

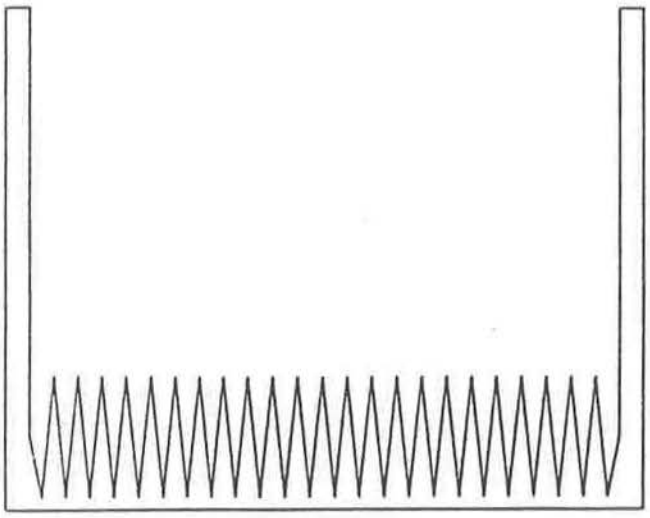

(a) A simple curve

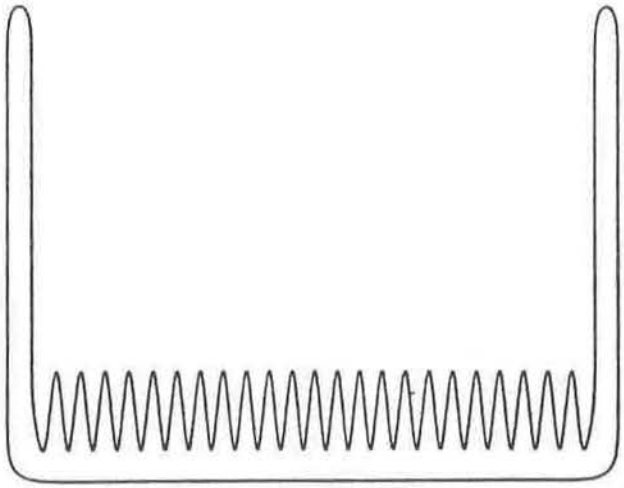

(b) Convolved with σ=4

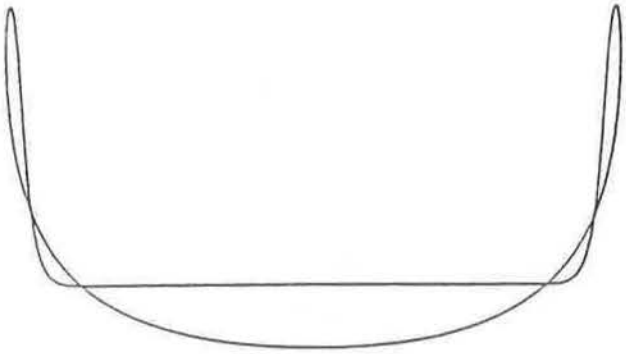

(c) Convolved with σ=16

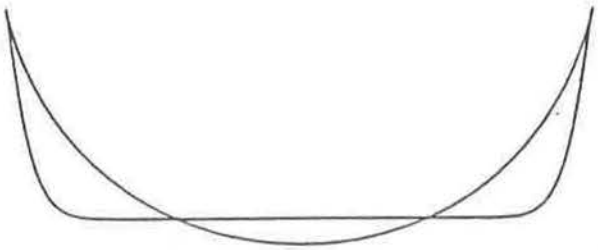

(d) Convolved with σ=25

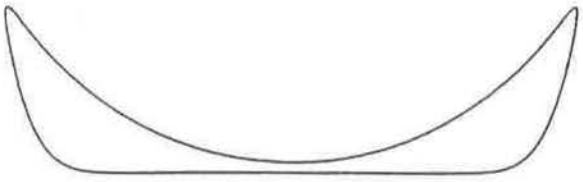

(e) Convolved with σ=32

(f) Convolved with σ=48

Figure 6.3. A simple curve during (regular) evolution

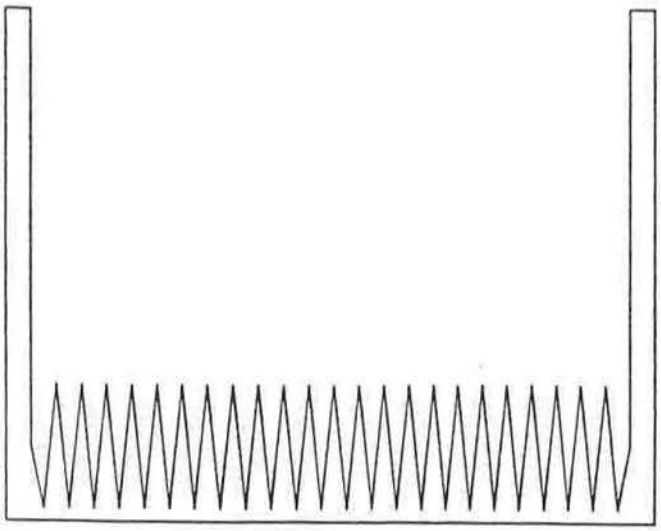

(a) A simple curve

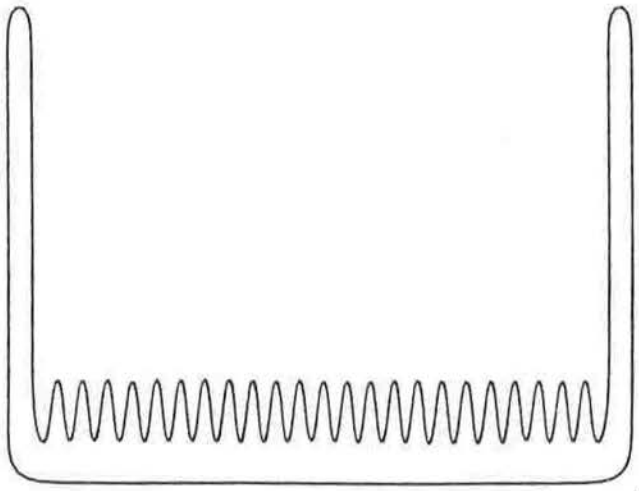

(b) After 3 iterations

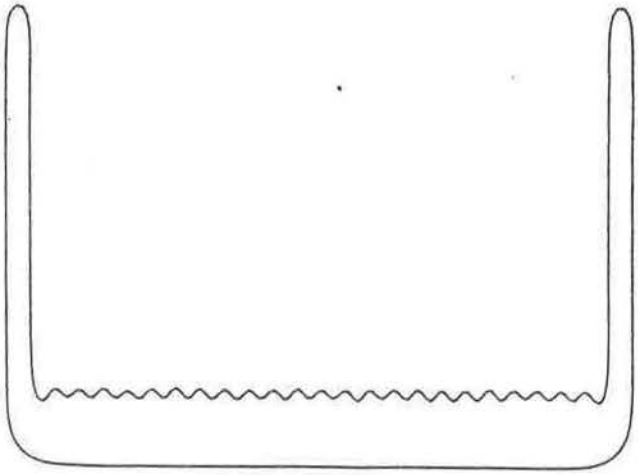

(c) After 6 iterations

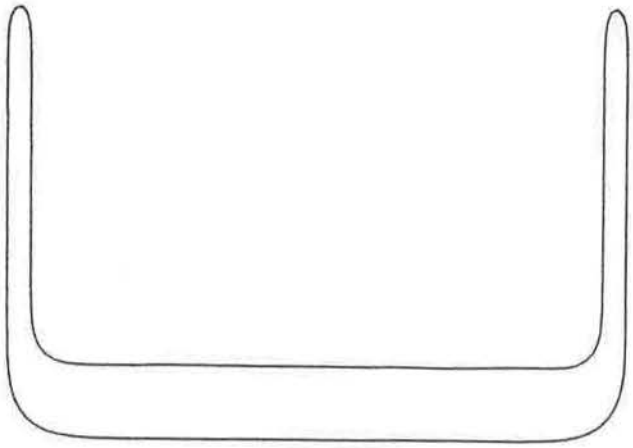

(d) After 10 iterations

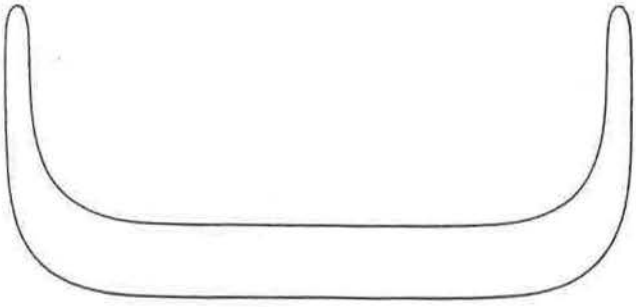

(e) After 30 iterations

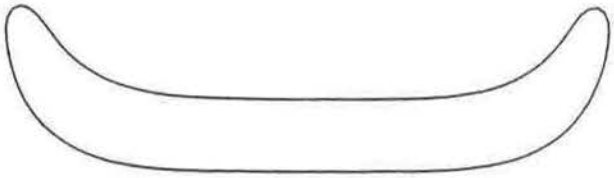

(f) After 50 iterations

Figure 6.4. A simple curve during arc length evolution